Universität Zürich[UZH]

USZ Universitäts Spital Zürich

Master thesis in physics

Nicolas Loizeau

Combined proton-photon radiotherapy: Optimal allocation of limited proton fractions for head and neck cancer patients

Supervisor: Prof. Dr. Jan Unkelbach

Tutor: Silvia Fabiano

Physik Institut, Zürich Universität, Schweiz

Department of Radiation Oncology, University Hospital Zürich, Switzerland

March 2020

Contents

Introduction

Ionizing radiations are used daily in cancer treatments. They ionize and excite atoms and molecules of biological tissues which may lead to the death of tumor cells but also healthy cells. The ultimate goal of radiotherapy is to deliver a high dose of radiation to tumor to eradicate it while maximally sparing the healthy tissues. External beam radiotherapy delivers ionizing radiations (e.g. photons or protons) to a patient lying on a treatment couch. Proton therapy (PT) reduces the dose in the normal tissue more than photon therapy (XT). Therefore, PT may have some advantage over XT such as gain in tumour control while respecting the dose constraints for the organs at risk (OARs) or reducing the radiation side-effects while delivering the same prescribed dose to the tumor. To date, most cancer patients are treated with XT while only a small percentage of patients are treated with PT, mainly because of the cost difference between XT and PT.

Although rapidly growing, proton therapy is a limited resource, which is not available to all patients who may benefit from it. For head and neck cancer, many OARs are located close to tumor volumes and PT has the potential to decrease the dose to these organs compared to XT. The central question of this work is how to make best use of these limited number of proton slots for a specific cohort of patients with head and neck cancer. To date, patients are optimally selected for either a complete PT treatment or a complete XT treatment. We investigate combined proton-photon treatments in which some fractions are delivered with protons and the rest with photons as an approach to optimally use the limited proton resources and maximize the benefit of PT at a population level (e.g. reduction of the side-effects). The goal of this work is to investigate if there is room for improvement with a combined proton-photon treatment compared to a single-modality treatment.

The background and the motivations of this work are detailed from chapters 1 to 3. The basic of PT and XT radiotherapy (Chapter 1), a short review of head and neck cancer treatment (Chapter 2) and the state of research on combined proton-photon radiotherapy (Chapter 3) are presented. The materials consisting of a data set of 45 head and neck cancer patients and Normal Tissue Complication Probability (NTCP) models are described in chapters 4 and 5. The methodologies to optimally allocate a limited number of proton slots over the given patient cohort are detailed in chapter 6. In chapter 7, we consider a clinic offering both photons and protons and a scenario in which only limited PT slots are available per day for treating head and neck cancer patients. We develop a daily slot allocation strategy in which protons slots are reassigned daily to patients who benefit the most and compare this strategy to an optimal PT patient selection.

1 Basic of radiotherapy

In this chapter, the basic of photon therapy and proton therapy are reviewed. The interactions of high energy photons and protons in matter are summarized in section 1.1. In section 1.2, the absorbed dose is defined and the dose deposited in water by photon and proton beams is described. In section 1.3, modern techniques of radiotherapy with photons and protons are detailed.

1.1 Photon and proton interactions in the matter

1.1.1 Photons

For a conventional XT treatment, high energy X-rays are delivered to the patient with energies up to 6 MeV or 15 MeV. The photons are indirectly ionizing radiations as they transfer energy to charged particles which then deposit energy in the matter [1]:

1. Firstly, X-rays may experience four types of interaction in the matter: the photoeffect, Compton effect, pair production and photonuclear interactions. The probabilities for each interaction to occur depend on the energy of the incident photon and the irradiated medium properties (e.g. the atomic number Z and the density ρ of biological tissues). These probabilities are summarized in Table 1. The main interactions occurring during XT are illustrated in Figure 2.

    - **Compton effect:** In the energy range for XT, the Compton effect is dominant ($\sim$ 99%). An incoming photon is interacting with an unbounded and stationary electron (the binding energy of the electron is neglected). The photon is scattered and transfers part of its energy to the electron, called the Compton electron. The higher the energy of the incident photon is, the more the Compton electron is directed in the forward direction.
    - **Photoeffect:** At lower photon energies (<100 keV), an incident photon interacts with a tightly bound orbital electron and is absorbed, while the orbital electron is ejected.
    - **Pair production:** An incident photon with an energy higher than 1.022 MeV can produce an electron–positron pair within the Coulomb field of an atom.
    - **Photonuclear reactions:** Photons with energy higher than 20 MeV may interact with the atomic nucleus resulting in an emission of a high energy neutron or proton and may transform the nucleus into a radioactive product.

2. Secondly, the released charged particles (secondary particles) such as the Compton electrons deposit energy in the matter through several ionizations and excitations.

Table 1 – Probabilities of photon interaction process as function of the energy of the incident photon. Adapted from Fritz-Niggli [2]

Energy	10 keV	200keV	2 MeV	20 MeV
Photoeffect	>99%	< 1%	<0.1%	-
Compton effect	-	>99%	$\sim$ 99%	$\sim$ 50%
Pair production	-	-	$\sim$ 1%	$\sim$ 49%
Photonuclear reactions	-	-	-	$\sim$ 1%

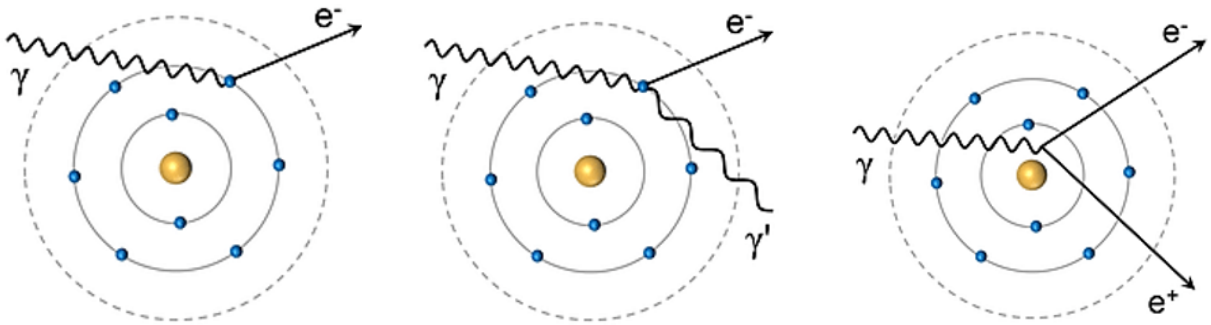

(a) Photoeffect **(b)** Compton effect **(c)** Pair production

Figure 2 – Photon interactions in matter: a) Photoeffect, b) Compton effect, c) Pair production. γ: incident photon, e^-: electron, γ': scattered photon, e^+: positron. Adapted from Soliman [3]

1.1.2 Protons

For a conventional PT treatment, protons with energy in the order of 70-200 MeV are used. As an energetic proton traverses matter, it may experience electromagnetic interactions (Coulomb interactions) and nuclear interactions [4]. These interactions are illustrated in Figure 3.

- **Electromagnetic interactions:** Protons experience Coulomb interactions with either the atomic electrons or the atomic nuclei. The energy loss of a proton comes mainly from the collisions with atomic electrons. Also, protons can be scattered by collisions with atomic nuclei, which determines the broadening of a proton beam. Soft collisions happen when protons transfer energy in the order of a eV to the atom and are deviated. Hard collisions happen when the energy transferred from the proton to the atom is sufficient to cause excitation or ionization.
- **Nuclear interactions:** Protons may interact with a nucleus and produce secondary particles (e.g. secondary protons, neutrons) in a non-elastic collision. This process is infrequent in the energy range of radiotherapy but must not be neglected.

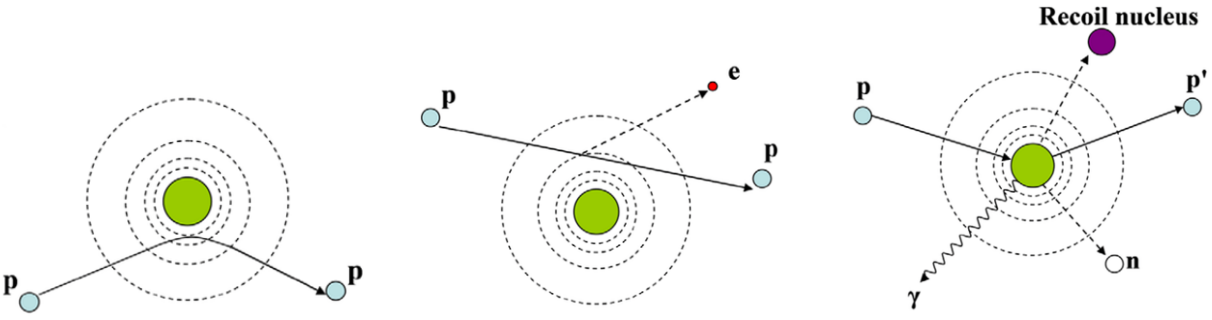

(a) Soft collision **(b)** Hard collision **(c)** Nuclear interactions

Figure 3 – Proton interactions in matter. Coulomb interactions with a) soft collision and b) hard collusion. c) Nuclear interactions. p: proton, e: scattered electron, γ: scattered photon, p': secondary proton, n: neutron. Adapted from Newhauser et al. [5]

1.2 Absorbed dose and depth dose curves

The absorbed dose D (Eq. 1) is defined as the mean energy dE deposited by ionizing radiation in a mass element dm and it' s measured in Gray [Gy].

$$D = \frac{dE}{dm} \qquad 1\ \text{Gy} = 1\frac{\text{J}}{\text{kg}} \tag{1}$$

The depth dose curves for 120 keV, 8 MeV and 22 MeV γ photons and 160 MeV p^+ protons in a water tank are illustrated in Figure 4.

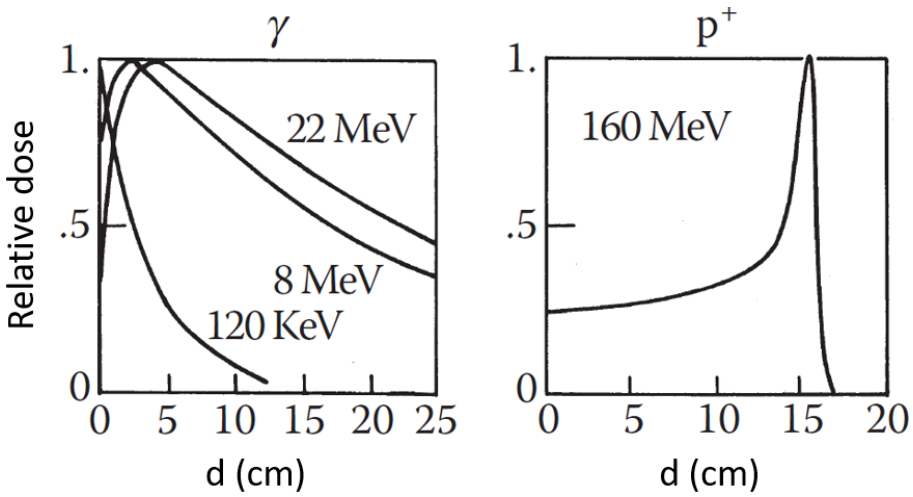

Figure 4 – Depth dose curves for 120 keV, 8 MeV, 22 MeV photon beams (left) and 160 MeV proton beam (right) in a water tank. Adapted from Paganetti [4]

For photons, the dose is proportional to the energy deposited by the secondary electrons. The dose build-up region is mainly caused by forward scattered Compton electrons. These electrons carry away energy from the interaction point and yield to a dose reduction near the surface called the skin-sparing effect. The range of Compton electrons and the probability for a Compton electron to be scattered in the forward direction increase with higher photon energies. So, the skin-sparing effect is higher for a 22 MeV photon beam than a 120 keV or 8 MeV photon beams. Then, the dose is decreasing exponentially with depth as the intensity of the photon beam is decreasing according to the Beer-Lambert law.

The Coulomb interactions of protons with atomic electrons mostly determine the shape of the proton depth dose curve. The Coulomb interactions with atomic nuclei has almost no impact on the depth dose curve. The linear collision stopping power S (Eq. 2) describes the rate of energy loss per unit path length $\frac{dE}{dx}$ for a charged particle resulting from the hard and soft collisions. According to the Bethe-Bloch formula, stopping power is proportional to $\frac{1}{v^2}$, z^2 and physical properties of the irradiated medium (e.g. Z, ρ), where v is the velocity of the incident particle and z the charge of the particle.

$$S = -\frac{dE}{dx} \propto z^2 \frac{1}{v^2} \tag{2}$$

As the collision stopping power is increasing while the protons are slowing down, a peak of the dose is occurring at the end of the proton's track called the Bragg peak. Not all the protons stop at the same depth even if they have the same initial energy. Therefore, the Bragg peak has a certain width of a few millimetres because of the statistical distribution of the proton tracks. This effect is called the range straggling. The position of the Bragg

peak depends on the initial energy of the proton beams and the medium in the beam path. The energy deposited as function of depth (i.e. depth dose curve) can be calculated by integrating the partial differential equation S over the depth.

The dose distributions for a 15 MeV photon beam and a 150 MeV proton beam entering a water tank from the left are illustrated in Figure 5. For the photon beam, the highest dose is located between 5 and 7 cm and Compton electrons deposit energy within a few millimetres from the central axis. The skin-sparing effect is observed in the entrance region. Photon beams with various angles are used to deliver a high and homogeneous dose to the tumor volumes. For a mono-energetic 150 MeV proton beam in a water tank, the Bragg peak is located at 15.8 cm. Therefore, a single proton beam can deliver a high dose to deep-seated tumors. Also, the lateral penumbra for proton and photon beams at large depth are roughly comparable.

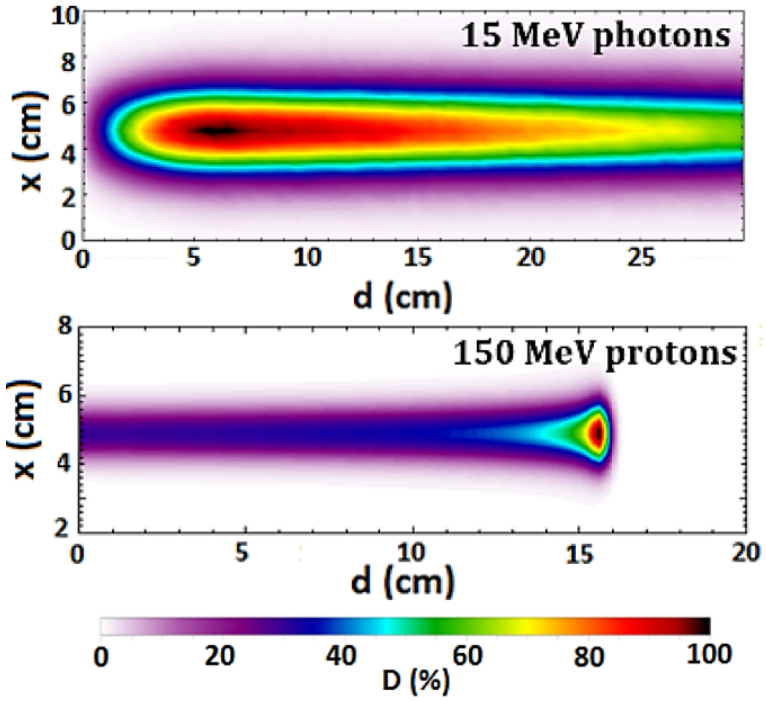

Figure 5 – Two dimensional dose distributions in a water tank for a 15 MeV photon beam (up) and a 150 MeV proton beam (down) coming from the left side. Adapted from Lagzda et al. [6]

A single mono-energetic proton pencil beam is not suited to treat a tumor, because the width of a proton pencil beam is in the order of a few millimetre which is too narrow to treat a tumor of a few centimetres. In PT, proton beams with various energies are used to deliver the dose homogeneously over the tumor volume. This is called the Spread Out Bragg Peak (SOBP) illustrated in Figure 6. The dose at the entrance region is increased by adding all the single Bragg peak curves. There is no skin-sparing effect compared to XT. To further optimize the dose distribution, multiple beam angles are used in PT.

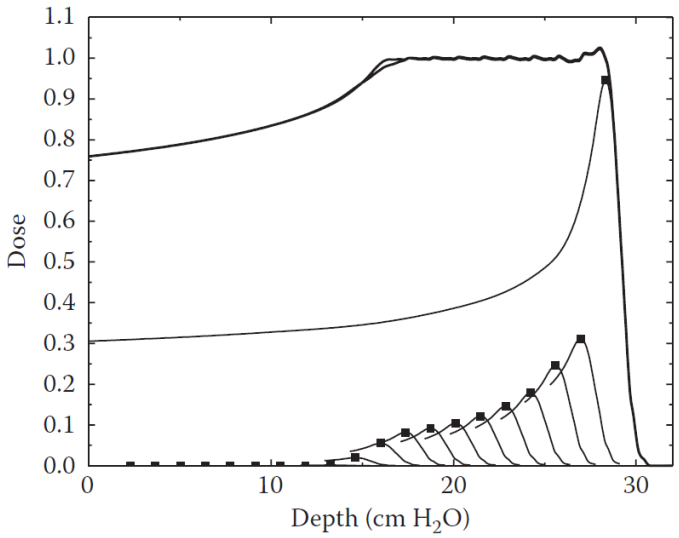

Figure 6 – Multiple proton beams with various energies form a Spread Out Bragg Peak (SOBP) in a water tank. Adapted from Paganetti [4]

An equivalent physical dose delivered by photons or protons does not mean that their biological effect is the same. For protons, the relative biological effectiveness (RBE) is defined as the ratio of the dose of the reference radiation D_{ref} (X-rays) to the proton dose D_p to produce the same biological effect.

$$RBE = \frac{D_{ref}}{D_p}|_{\text{same biological effect}} \tag{3}$$

Current clinical practice uses a constant RBE for protons of 1.1 [4]. Thus, the prescribed dose delivered by proton is 10% lower than for photons. This biologically weighted dose is given in GyE (Gray Equivalent).

1.3 State of the art of radiation therapy

Cancer patients treated with radiotherapy undertake a computed tomography (CT) scan, and possibly also a magnetic imaging resonance (MRI) scan and a positron emission tomography (PET) scan. A three dimensional (3D) image representing the electron densities of the tissues is obtained from the CT scan. Organs with similar electron density can be distinguished with the MRI scan which allows to differentiate the magnetization properties of various organs. The PET scan makes it possible to localize the tumor with an activity map of a radionuclide (e.g. ^{18}F) attached to a tracer (e.g. fluorodeoxyglucose (FDG)) which is administered to the patient. These three scans are overlaid to represent a 3D image of the patient anatomy and an experienced physician contours the organs at risk (OAR) and the tumor volumes (e.g. primary tumor, lymph node metastasis) based on that image. Tumor contours and standard of care prescription for head and neck (HNC) patients are detailed in section 1.3.1. A radiation oncologist prescribes the dose to the tumor volumes, dose constraints to OAR, and fractionation scheme. Using the electron densities and clinical software for treatment planning, an optimal 3D dose distribution is calculated to be delivered to the patient. To evaluate the quality of a treatment plan, some parameters are measured such as the dose coverage and conformity of the dose distribution to tumor volumes, the fulfilment of the dose constraints for the OAR. Once the treatment planning is accepted by the physician, the radiotherapy treatment can start. Modern radiotherapy treatments with photons and protons are described in section 1.3.2 and 1.3.3.

1.3.1 Tumour contours and standard of care treatment

Figure 7 illustrates the target volume concepts as defined in the International Commission on Radiation Units and Measurements (ICRU) reports. ICRU reports No. 50 [7] and No. 62 [8] provide guidance on dose prescription. The gross tumor volume (GTV) is the "solid tumor". The clinical target volume (CTV) is an extension of the GTV to account for microscopic disease. The internal target volume (ITV) is a margin for variations in size and position of the CTV relative to the patient's reference frame. The planning target volume (PTV) takes into consideration all possible geometrical variations such as set-up uncertainties and potential organ movement to ensure that the prescribed dose is absorbed in the CTV.

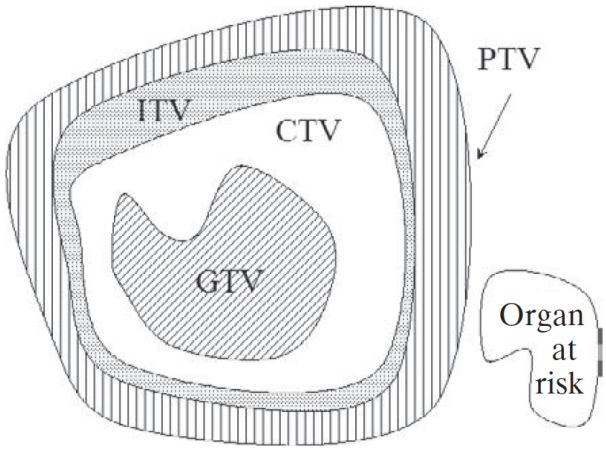

Figure 7 – Tumor contours for treatment planning: *GTV*: Gross Tumor Volume, *CTV*: Clinical Target Volume, *ITV*: Internal target volume, *PTV*: Planning Target Volume. Adapted from Podgorsak and Kainz [1]

For HNC patients, a standard of care treatment is defined such that 54 Gy are delivered in the PTV and 70 Gy are delivered in the GTV in 30 fractions. Cancer patients usually receive one fraction every working day (5 days per week) for 6 weeks.

1.3.2 Intensity Modulated Photon Therapy

A medical linear accelerator (Linac) produces high energy X-rays in the range of 6 to 15 MeV by accelerating electrons which are then producing photons in a target by Bremsstrahlung. A Linac rotates around the patient and delivers radiation fields from several angles to achieve a conformal and homogeneous dose distribution in the tumor volumes. Nowadays, Linacs are equipped with multileaf collimators (MLCs), illustrated in Figure 8, that consists of a large number of highly absorbing tungsten 'leaves' that can be moved against each other and thereby shape the projection of the tumor volume.

MLCs also facilitate the delivery of intensity modulated radiotherapy (IMRT). In IMRT, the radiation field to the photon beam is divided into beamlets. The intensity of the beamlet that goes through organs at risk must be reduced and the intensity of the beamlet that sees primarily the target volume must be increased. All the beamlets are simultaneously optimized in IMRT, so that the resulting dose per beam is not uniform. By superimposing all the beams from different angles, an homogeneous dose distribution in the target volume is obtained [9].

The step-and-shoot mode is an IMRT delivery technique which consists of a succession of discrete field openings and turns the beam off while the MLC leaves move to their next position.

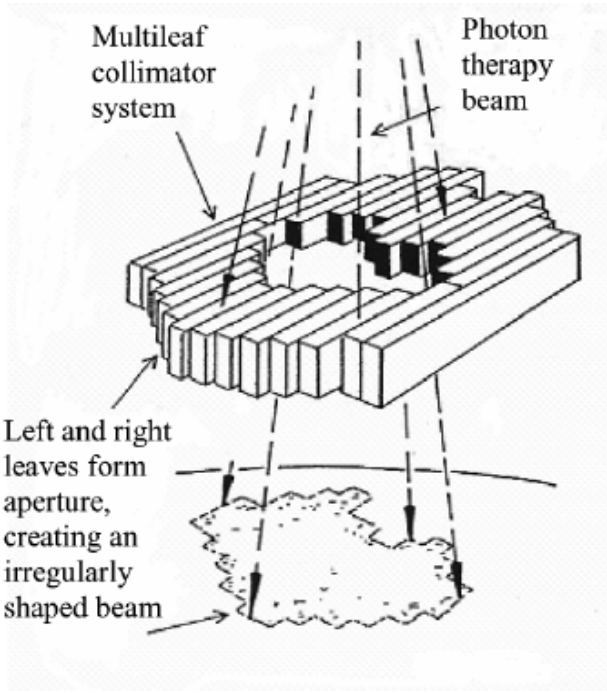

Figure 8 – Scheme of a photon beam passing through multileaf collimators (MLCs) system, which shape the projection of the tumor volume. Adapted from Romeijn et al. [10]

To date, around 12'000 conventional X-Ray machines are operational in the world [11].

1.3.3 Intensity Modulated Proton Therapy

To reach deep-seated tumors in PT, protons must be accelerated between 70-200 MeV with a cyclotron or a synchrotron. The spot-scanning is an intensity modulated proton therapy (IMPT) delivery technique. In this technique, the protons are focused into a pencil beam of 5 to 7 mm width [12]. The "spot" represents the high dose delivered by the proton pencil beam in the Bragg peak region. The proton energy of a pencil beam is varied to produce a resulting SOBP in one direction. Figure 9 illustrates ten incident proton pencil beams which are directed in the tumor and the positions of their Bragg peak cover the entire tumor. Each single spot is delivered one after the other. Gantries can steer the proton beams in the patient direction from a range of angles. Using three to seven beam angles, the positions and the intensities of these high dose spots are optimally modulated in three dimensions to cover the entire tumor with an homogeneous and conformal dose distribution while sparing maximally healthy tissues [13].

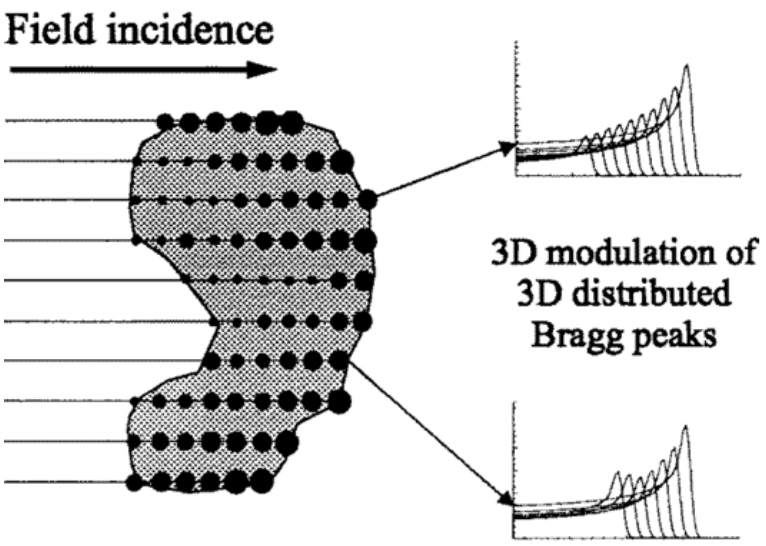

Figure 9 – Spot-scanning technique. Tumor volume is covered by 10 proton beams coming from the left side. Positions of solid circles represent individual Bragg peak positions and circle diameters symbolize their relative intensities. The depth dose curves for two proton beams with various energies are indicated on the right hand side. Adapted from Lomax [14]

82 proton therapy centres with one, two or three treatment rooms are operational worldwide [15]. They are build in multistorey buildings to accommodate gantries with wheels of diameter of 10 meters weighing up to 200 tons. There are also smaller gantries with a proton fixed beamline. The number of proton center exponentially increased during the last 80 years as shown in Figure 10 [16]. Like with XT concrete shields are necessary to protect the medical staff from secondary particles (e.g. stray neutrons).

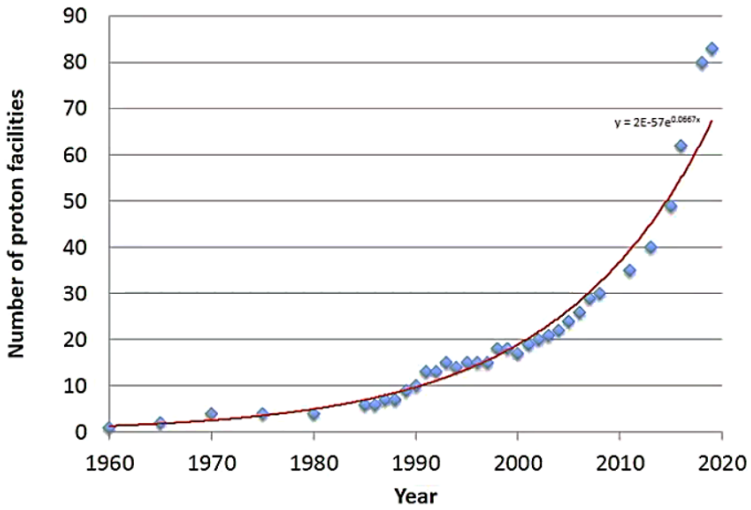

Figure 10 – Exponential increase of proton facilities worldwide during the last 80 years. Adapted from Bortfeld [17]

2 PT for head and neck cancer patients

In this work, we investigate a cohort of head and neck cancer (HNC) patients. A brief general overview of the most common type of HNC is presented in section 2.1. The pros and cons for treating HNC patients with XT or PT are presented in section 2.2. With the goal to deliver PT to patients who benefit the most, a methodology to select HNC patients for PT has been developed in the Netherlands. This patient selection approach is detailed in section 2.3.

2.1 Head and neck squamous cell carcinoma

The regions where head and neck cancers can develop are the oral and nasal cavity, paranasal sinuses, pharynx, larynx, trachea, esophageous and salivary glands [18]. These regions are illustrated in Figure 11. Squamous cells are thin and flat epithelial cells which are present in the human aero-digestive tract. A cancer that originates from a squamous cell is called squamous cell carcinoma. Head and neck squamous cell carcinoma (HNSCC) is a type of cancer that arises commonly in the oral cavity, pharynx and larynx and represents 95% of all types of head and neck cancers [18]. Examples of symptoms of HNSCC are ulcers, pain and bleeding in the mouth, sinus congestion that does not clear, sore throat and enlarged lymph nodes. HNSCC are the sixth most common cancer worldwide [19]. The main risk factors to develop HNSCC are smoking and excessive alcohol consumption which implicate 75% of HNSCC patients. Infection of human papillomavirus (HPV) is also a risk factor and implicates less the 25% of HNSCC patients. HNSCCs have a yearly incidence of 600,000 cases worldwide and 40–50% of patients with HNSCC will survive at 5 years [20], [21]. Experienced physicians decide for the most favourable treatment option for each patient, which depends on the tumor location and tumor stage. HNSCC patients with stage I or II are usually treated with surgery or radiotherapy. They represent about one-third of HNSCC patients. It is possible to cure up to 90% of patients with stage I and 70% of patients with stage II [22]. HNSCC patients with stage III or IV are in a locally advanced stage. They can be treated with chemotherapy, surgery, radiotherapy or a combination of these treatments (e.g. chemoradiotherapy). Patients can develop side-effects due to radiation, which can seriously impact their quality of life as the HNSCCs are close to many sensitive organs such as the brain stem, spinal cord, salivary glands (parotids) or larynx. Examples of these complications are mouth dryness (xerostomia), inflammation of the mucous membranes in the oral cavity (oral mucositis), swallowing dysfunction (dysphagia), larynx-based and pharyngeal constrictor muscles - based aspiration.

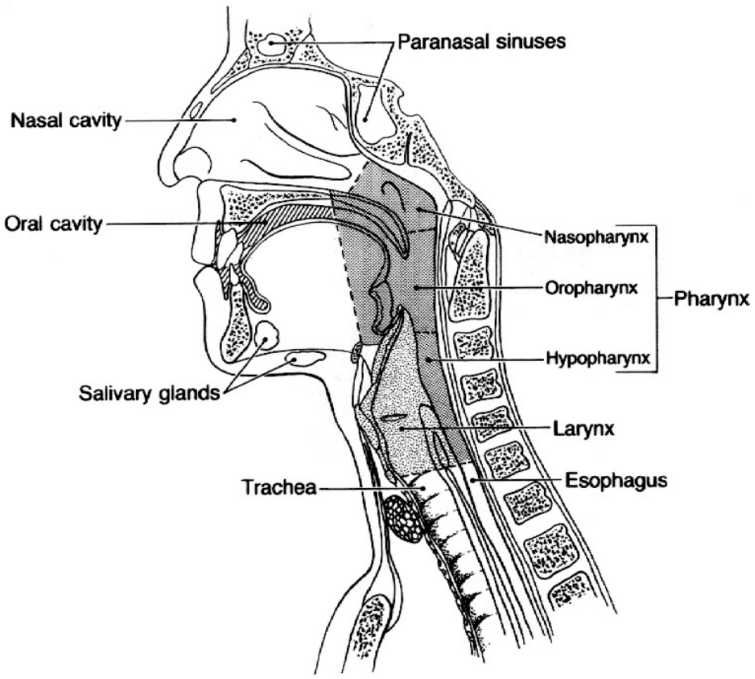

Figure 11 – Illustration of the head and neck cancer regions. Adapted from Vokes et al. [18]

2.2 Pros and cons of proton therapy for HNSCC

IMPT offers some general advantages over IMRT. Previous comparative studies demonstrated that these advantages were also valid for locally advanced HNSCC patients [23]–[27]:

- IMPT offers similar or even better dose coverage and homogeneity to the PTV compared to IMRT
- IMPT has the potential to decrease the integral dose compared to IMRT which results in decreasing the complication risks after radiotherapy
- IMPT offers a potential dose escalation in the target volume while respecting normal tissue dose constraints which can improve the tumor control
- IMPT significantly reduces the estimated risk of secondary cancer induction compared to IMRT

.

In this study, we focus on the potential benefit of IMPT in terms of complication risks. Normal Tissue Complication Probability (NTCP) models translate dose parameters (e.g. mean dose) of organs at risk to estimated risks for radiation-induced side effects. For example, for HNSCC patients, irradiation of the salivary glands (parotids) can lead to dryness of the mouth (xerostomia). The probability of this toxicity can be described by the NTCP model for xerostomia (section 4.3), which depends on the mean dose to the contralateral parotid gland. IMPT has the potential to reduce the mean dose to the contralateral parotid gland compared to IMRT. In this case, the NTCP value for IMPT ($NTCP^{IMPT}$) is lower than the NTCP value for IMRT ($NTCP^{IMRT}$). The magnitude of this NTCP reduction is given by the $\Delta NTCP$ value (Eq. 4) illustrated in Figure 12.

$$\Delta NTCP = NTCP^{IMRT} - NTCP^{IMPT} \tag{4}$$

For example, a $\Delta NTCP$ of 16% for xerostomia is feasible if a patient receive a mean dose to the contralateral parotid gland of 34 Gy with IMRT and 25 Gy with IMPT. Due to the shape of the NTCP curve, an equivalent decrease of the mean dose from 24 Gy with IMRT to 15 Gy with IMPT leads to a smaller $\Delta NTCP$ value of 10%.

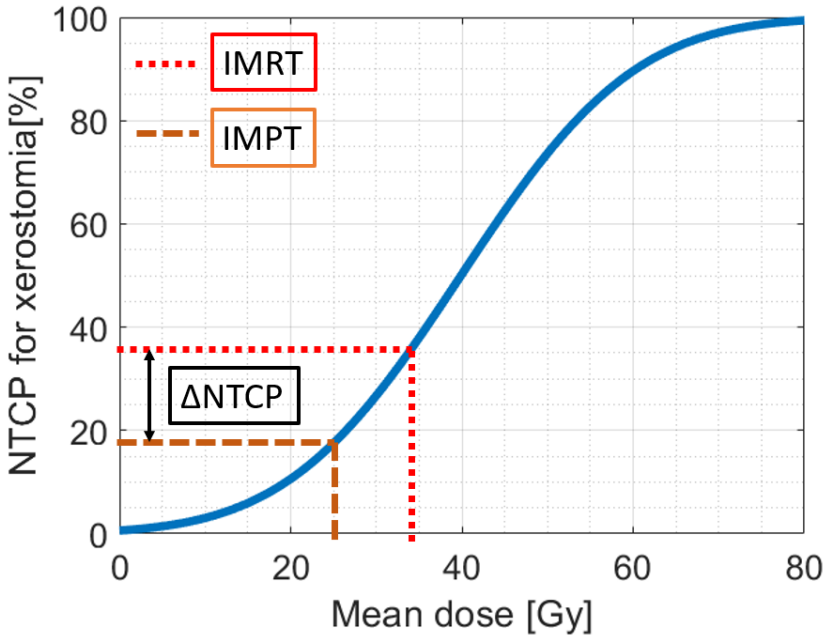

Figure 12 – Normal Tissue Complication Probability (NTCP) model for xerostomia [28] as function of the mean dose to the contralateral parotid gland. Example of a ΔNTCP value of 16% with mean doses of 34 Gy with IMRT and 25 Gy with IMPT

On the other hand, PT is less available and more costly compared to XT. For these reasons most cancer patients are treated with XT. Peeters et al. [29] attempted to investigate the cost for external beam radiotherapy with photons and protons. Based on literature about cost and cost-effectiveness for four cancer indications (prostate, lung, head and neck, and skull-base chordoma), they estimated the overall cost ratio to photons to be 3.2 for protons. For head and neck cancers, the average number of fractions and their corresponding estimated costs per treatment are shown in Table 2. For this cancer indication, the cost ratio to photons is 3.4 for protons.

Table 2 – Average number (and range) of fractions per treatment and costs per treatment for HNC patients for PT and XT. Adapted from Peeters et al. [29]

Treatment modality	Number of fractions per treatment	Costs per treatment [€]
PT	32 (26-40)	39,610 (32'180–49'510)
XT	33 (25-35)	11,520 (8'730–12'220)

Efforts are made to reduce the cost and the size of proton therapy. Bortfeld and Loeffler [16] suggested to build more compact PT systems and broaden health-care coverage. About 12 'miniaturized' proton facilities are operational. For example, the Boston Massachusetts Hospital built one of this 'miniaturized' proton facility in which one proton treatment room fits the space of two conventional photon treatment rooms [17].

2.3 Model-based PT patient selection for HNSCC

Langendijk et al. [30] described a methodology to select patients for PT based on expected clinical benefit, called model-based PT patient selection. This methodology aims to select the patients who could potentially decrease probability of the radiation-induced side effects the most with IMPT compared to IMRT, while delivering a similar dose to the target volume. This method has been validated by the Dutch health authorities. For HNC patients, a Dutch national protocol [31] describes the criteria for a patient to be eligible for PT:

Firstly, a photon plan is created. Then, the need to create a proton treatment plan is determined. It doesn't make sense for every HNC patient to have a treatment plan comparison as it is time-consuming. The NTCP profile for the photon treatment plan for each HNSCC patient is checked successively and a proton treatment plan is created as soon as one of the following criteria is met:

1. The $NTCP^{IMRT}$ value for dysphagia with at least grade II is higher than 10%
2. The $NTCP^{IMRT}$ value for moderate-to-serious dry mouth is higher than 18% if no xerostomia was present prior to treatment
3. The $NTCP^{IMRT}$ value for dysphagia with at least grade II is higher than 5% and the $NTCP^{IMRT}$ value for xerostomia is higher than 13%
4. The $NTCP^{IMRT}$ value for tube feeding dependency is higher than 5%

Secondly, for the HNC patients who fulfil one of these criteria, a proton treatment plan is created using the same planning CT and contours as for the photon treatment plan. Relevant $NTCP$ values for protons are calculated. A treatment plan comparison is performed in which several $\Delta NTCP$ values (Eq. 4) are calculated. Patients are eligible for PT as soon as their $\Delta NTCP$ values fulfil one of following criteria, which are checked successively:

1. The $\Delta NTCP$ value for dysphagia with at least grade II is higher than 10%
2. The $\Delta NTCP$ value for xerostomia for moderate-to-serious dry mouth is higher than 10%
3. The sum of the $\Delta NTCP$ for xerostomia and for dysphagia is higher than 15% and if both $\Delta NTCP$ are higher than 5%
4. The $\Delta NTCP$ value for tube feeding dependency is higher than 5%

The HNSCC patients who don't meet any of these criteria are assigned to XT treatment.

3 Combined proton-photon radiotherapy

Investigating combined proton-photon radiotherapy has various motivations. So far, combined treatment was investigated to obtain higher quality plans than with a single-modality treatment and to make proton therapy more available. An overview of the research on combined treatment is presented in section 3.1. In this work, we investigate combined proton-photon radiotherapy in the context of limited proton resources. The aim and rationales of this thesis are explained in section 3.2.

3.1 Overview of research on combined treatment

Combined radiotherapy was investigated to obtain higher quality plans than single-modality radiotherapy. In this context, studies demonstrated the benefit of a) adding a proton boost to an IMRT plan and b) optimizing simultaneously the proton and the photon plans. A recent study on combined proton-photon radiotherapy demonstrated c) a new-approach to make proton slots more available and affordable.

a) Proton boost added to an IMRT plan

   Most of combined proton-photon treatment performed in clinic delivers a proton boost to tumor regions with high risk of recurrence. Basically, the physician decides the number of proton and photon fractions a patient should receive. The goal of delivering proton boost fractions is to increase the local control probability of the tumor. Combs and Debus [32] reviewed clinical data and current clinical trials for treatment with heavy charged particles, in particular combined treatments with photons, protons or carbion-ions. Jakobi et al. [27] investigated the potential benefit for a combined treatment for HNSCC patients in which 11 proton fractions are delivered with a sequential boost and 25 photon fractions are delivered with a base plan. They concluded that protons delivered only in boost plans reduce the NTCP values for dysphagia or xerostomia by at least 10% for 15% of the patients while the same reduction of risk was observed for 50% of the patients assigned to pure IMPT.

   To date, the IMPT and IMRT plans are separately optimized and each plan delivers a conformal and homogeneous dose to the tumour. As an extension to this approach, Eikelder et al. [33] investigated an optimization approach for photon and proton plans for a data set of 17 patients with liver tumors. Here are two reasons to investigate it [33]:

   (1) Due to the range uncertainties of the Bragg peak, an OAR in proximity (OAR_{prox}) to the tumor could receive locally a high dose with PT compared to XT for which the OAR_{prox} could be irradiated completely with a low dose. In addition to this, a distant OAR (OAR_{dist}) to the tumor receives no dose with PT (if the proton beam is not directed to the OAR) while the OAR_{dist} receives a low dose with XT. Assuming that PT is more beneficial for the OAR_{dist} and XT is more beneficial for the OAR_{prox}, combining PT and XT can outperform the single-modality treatment.

   (2) If a proton plan is better than a photon plan but all of the fractions cannot be delivered with protons, the proton dose per fraction could be increased while limiting the dose to normal tissues compared to photon fractions. It is possible to do it for cancer in which almost no normal tissues are present in the target volumes (e.g. liver tumor).

Eikelder et al. first obtained the IMRT and IMPT plans, which were separately optimized. Then, they allowed for the proton and photon dose per fraction to be different by optimizing the dose per fraction and the number of proton and photon fractions based on the cumulative biologically effective dose (BED) which accounts for the fractionation effect. They compare their results with an optimum proton treatment. Here are summarized the main results:

- For 5 patients, there is a substantial improvement of the BED for the optimized combined plans. For 3 of 5 patients, less proton fractions are used than the optimum proton treatment.
- For 9 patients, combined-modality treatment offers near-optimal irradiation as pure IMPT treatment but uses less proton fractions .
- For 3 patients, the optimal irradiation is with pure IMPT.

For specific patients, combined proton-photon radiotherapy with an optimized treatment plan offers an alternative treatment with less proton fractions and is marginally worse than an optimal proton treatment.

b) Simultaneous optimization of the IMRT and IMPT plans

An extension of Eikelder's method was developed by Unkelbach et al. [34]. They investigated a novel treatment that simultaneously optimizes the photon and proton doses with the goal to optimally use a limited number of proton fractions. In this study, photons are used to treat target volumes overlapping OARs while protons hypofractionate remaining parts of target volumes. With this approach, the proton and photon treatment plans deliver individually an inhomogeneous dose to the tumour volume, unlike Eikelder's method in which the individual proton and photon plans deliver an homogeneous dose to the target volumes. For a sacral chordoma patient, they developed a simultaneous optimization treatment with 10 IMPT and 20 IMRT fractions which was compared to an optimal proton treatment with 30 fractions. They demonstrated that an integral dose reduction in the gastrointestinal tract of 50% is achievable with the simultaneous optimization treatment compared to a 30 IMPT fractions treatment. With 10 IMPT and 20 IMRT fractions delivering the same dose to the target, the integral dose reduction is 33%.

Another approach for a combined treatment was developed by Goa et al. [35]. They simultaneously optimized the proton and photon variables based on the joint physical dose for two prostate and two HNC cancer patients with the goal to improve on single photon and proton plans by taking into account treatment uncertainties. With this approach, tumor volumes would not receive the same dose with the photon and proton plans. So, an additional objective was added to make the photon dose and proton dose in the tumor homogeneous. By adding together the optimized proton and photon plans, they obtained an uniform dose coverage in target volumes with similar dose per fraction as conventional single proton and photon plans. Here, the optimized proton and photon fractions would be separately delivered.

c) Combined treatment with a proton fixed beamline

To reduce the size and cost for PT, Fabiano et al. [36] developed a new approach of combined proton-photon radiotherapy in which the proton and photon doses are delivered in the same fraction. In this study, they suggested to integrate a fixed proton beamline with a standard Linac and a rotating couch allowing for different

position of the patient into a conventional bunker. A fixed horizontal proton beamline is smaller and less expensive than PT with a gantry. However, the dose distribution for radiotherapy with a proton fixed beamline is not as good as a dose distribution for PT with a gantry, because the proton beam is limited to an horizontal plane. Therefore, a standard Linac can be installed in the same treatment room as the proton fixed beamline to achieve an optimal dose conformity. In this situation, the proton and photon doses are simultaneously optimized [34]. Fabiano et al. [36] demonstrated for three HNC patients that this innovative approach of combined treatment improves on single-modality IMRT and fixed proton beamline.

3.2 Aim of this study

Although rapidly growing (Fig. 10), PT is a limited and costly resource, which is not available to all the patients who may benefit from it. The aim of this master thesis is to investigate combined proton-photon treatment as an approach to optimally use the limited PT resources and maximize the benefit of PT at a population level. Here, we consider combined proton-photon treatment in which some fractions are delivered with protons and the rest with photons. Also, we consider the dose per fraction and the number of fractions to be fixed. For HNC, normal tissues are within the elective target volumes and must be protected with fractionation, unlike liver tumors in which it is possible, in some case, to hypofractionate the tumor volumes (see section 3.1). Three rationales motivate combined proton-photon radiotherapy in the context of limited proton resources for HNC patients.

- The first reason that combined treatment with an optimal allocation of proton slots would be beneficial for a population of patient comes from the shape of the NTCP curve. By assuming that a patient would receive a pure XT treatment, delivering one proton fraction instead of one photon fraction decreases the NTCP value (e.g. for xerostomia). On the convex part of the NTCP curve (Fig. 12), the first proton fractions are the most beneficial while additional proton fractions lead lower improvement in term of NTCP value.

- Based on previous studies, patients could benefit from a base or a boost plan delivered with protons and the other plan delivered with photons.

- The PT patient selection strategy in which patients are assigned either to pure PT or XT based on the potential benefit for individual patient face a trade-off between leaving slots unused or blocking slots for future patients with higher benefit.

In chapter 4, a data set of IMRT and IMPT plans of 45 HNSCC patients is detailed and relevant NTCP models used in this study are presented. Here, the IMRT and IMPT plans are separately optimized. In chapter 5, two treatment schemes are obtained which mimic a standard of care treatment and the NTCP values for combined proton-photon radiotherapy are defined. In chapter 6 we develop methods to distribute the limited proton slots over the 45 HNSCC patients optimally in order to maximize the overall benefit of PT in terms of complication risks (NTCP models). We investigate the first two rationales to see if there is room for improvement with combined treatment with respect to an optimal single-modality treatment. In chapter 7, we consider a clinic offering both photons and protons and a scenario, in which only limited proton slots are available per day for treating HNSCC patients. We develop a new strategy to make an optimal use of all proton slots called the daily slot allocation and we compare this method with a PT patient selection strategy.

4 Dataset of 45 locally advanced head and neck cancer patients

For this study, a cohort of 45 patients with locally advanced head and neck squamous cell carcinoma (HNSCC) in different locations was obtained from OncoRay (National Center for Radiation Research in Oncology at Dresden, Germany). These patients were treated between 2006 and 2013 at the Dresden University Hospital. Most recurring HNSCC develop at the site of the initial primary tumor volume after a standard of care radiotherapy. A treatment intensification with a radiation dose escalation (DE) may improve patient outcome while it may increase the risk of toxicities in healthy tissues. Therefore, Jakobi et al. [37] investigated this patient cohort in a study whose aim was to compare the benefit of two DE levels (2.3 and 2.6 GyE per fraction) in terms of tumor control probabilities (TCP) and normal tissue complication probabilities (NTCP). They created, for both DE levels and all HNSCC patients, the IMRT and IMPT treatment plans presented below. They found out that the 2.6 GyE DE level increases the TCP by 10% while it increases slightly the considered NTCP values in regards to the 2.3 GyE DE level [37]. In an other study [38], Jakobi et al. compared the IMRT and IMPT plans of these patients in terms of NTCP to identify the patients who may benefit more than others from IMPT based on the tumor sites. In section 4.1 and 4.2, the treatment schedule and the treatment planning of these studies are detailed. In section 4.3, the NTCP models used in this study are presented.

4.1 Treatment schedule

The treatment schedule allowing for two DE levels was based on a baseline FDG-PET/CT and an adaptive FDG-PET/CT taken in the fourth week of treatment. The simultaneous integrated boost (SIB) technique applies a non-uniform dose distribution by increasing the dose in specific tumor volumes. It increases tumor control while limiting the increase of the complications risks [38]. The OARs and relevant structures were contoured by an experienced physician. The gross tumor volumes were contoured for the primary tumor GTV-T and involved lymph nodes GTV-N. SIB volumes (GTV_{SIB}) were defined such that they represent either the GTV-T if patients have a node measuring less than 6 centimetres or the union of the GTV-T and GTV-N if patients have a node larger than 6 centimetres. Planning target volumes including extensions of GTV-T (PTV-T), GTV-N (PTV-N), plus elective nodal target volumes were contoured for the baseline PET/CT scan (PTV_{all}). Planning target volumes for the adaptive PET/CT scan (PTV_{adapt}) are geometrical adaptations of the PTV-T and PTV-N. An additional SIB volume ($GTV_{SIB,adapt}$) was contoured based on the adaptive PET/CT scan. For both IMRT and IMPT plans, Jakobi et al. [37] defined a treatment schedule with 3 series (Fig. 13). Phase 1 was planned such that 10 fractions of 2 GyE are delivered uniformly in the PTV_{all}. Phase 2 was planned such that 15 fractions of 2 GyE are delivered in the PTV_{all} plus DE levels of 2.3 or 2.6 GyE in the GTV_{SIB}. Phase 3 was planned based on the adaptive PET/CT such that 11 fractions of 2 GyE are delivered in the PTV_{adapt} plus DE levels of 2.3 or 2.6 GyE in the $GTV_{SIB,adapt}$. Consequently, target doses were 50 GyE for PTV_{all} and 22 Gy for PTV_{adapt} (72 GyE in total) whereas the SIB volumes were escalated to a dose of 80 GyE or 88 GyE [38].

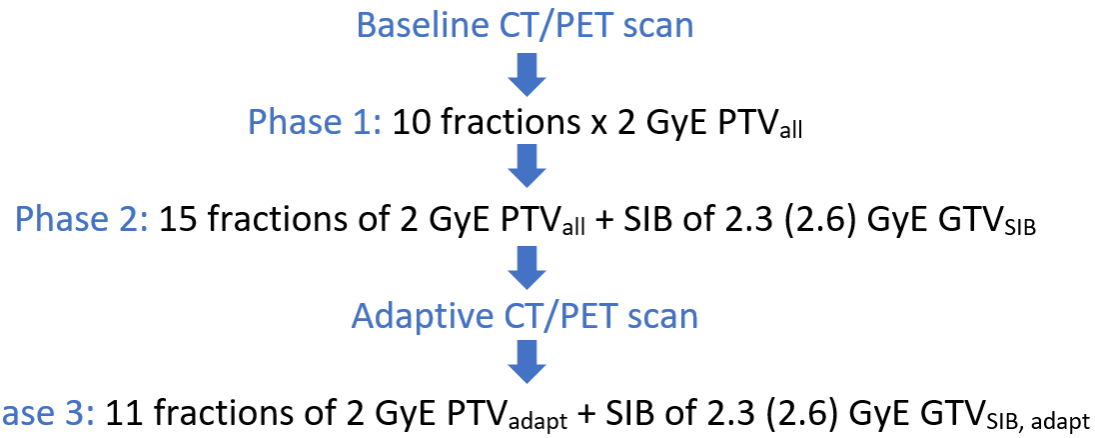

Figure 13 – Treatment schedule for the 45 HNSCC patients for IMRT and IMPT adapted from Jakobi et al. [37]

4.2 Treatment planning

For both proton and photon plans, a list of the main planning goals and constraints is shown in Table 3 in priority order for the study on the treatment intensification [37]. The maximum dose (D_{max}) to the spinal cord, the brain stem and the brachial plexus should not exceed 45 GyE, 54 GyE and 72 GyE, respectively. At least 95% of the PTVs and the SIB volumes have to be irradiated with more than 95% of the prescribed dose (V_{95}). Volumes which exceeded 107% (V_{107}) of the prescribed dose was minimized but accepted if the condition V_{95} in the GTV_{SIB} was fulfilled. The mean dose D_{mean} of at least one parotid gland should be lower than 26 GyE.

Table 3 – Goals and constraints of organs at risk and tumor volumes in priority order adapted from Jakobi et al. [38]

Organs at risk	Quantities	Values
1. Spinal cord	D_{max}	45 GyE
2. Brain stem	D_{max}	54 GyE
3. Brachial plexus	D_{max}	72 GyE if next to the PTV, otherwise 60 GyE
4. Parotid gland	D_{mean}	<26 GyE (at least for one parotid)
Target volumes		
1. PTV (72 GyE)	V_{95}	95% of prescribed dose
2. GTV_{SIB} (79.8-87.6 GyE)	V_{95}	95% of prescribed dose

Jakobi et al. created the IMRT and IMPT plans for every patient. For the IMRT plans, the step-and-shoot IMRT technique was used with 6 MeV photon beams and seven equally spaced and coplanar beams for Phase 1 and Phase 2. For Phase 3, the number of beam angles was reduced to five for one-sided PTV_{adapt}. For the IMPT treatment plan, the

protons were incident from with 3 beam angles: 40°, -40°and 180°by default. If needed, these angles were adapted for individual patient anatomy.

The IMRT and IMPT dose distributions with a DE level of 2.3 GyE of one transverse CT slice for one representative patient are shown in Figure 14. The IMPT dose distribution reduces the integral dose to normal tissues and delivers a similar conformal dose to tumor volumes compared to the IMRT plan.

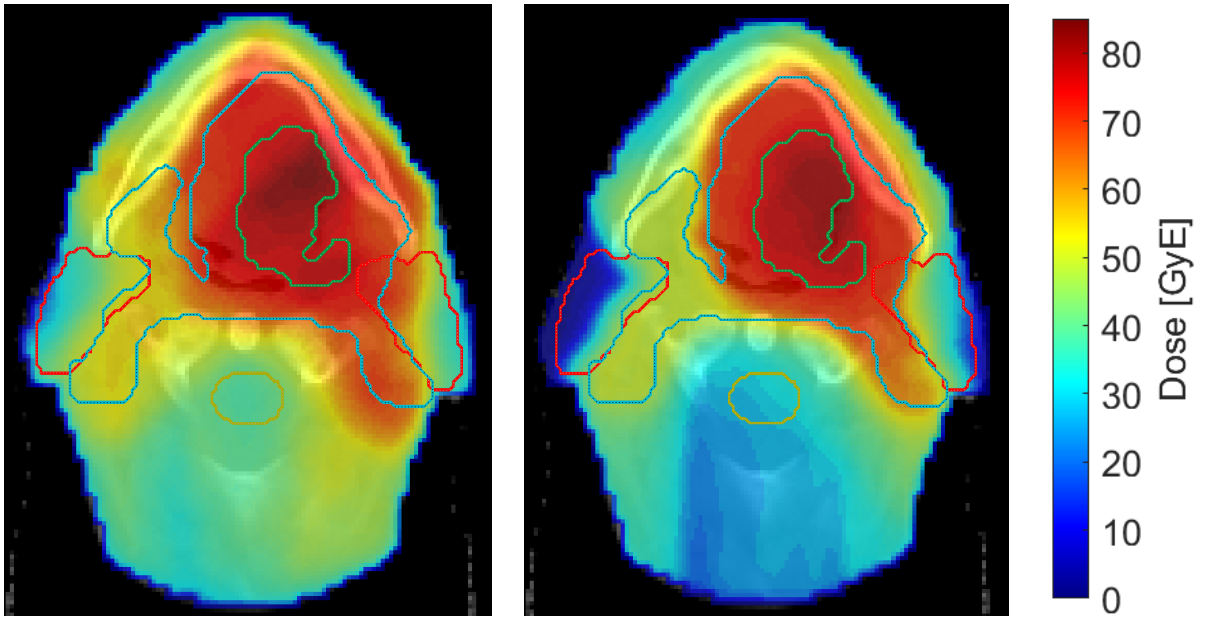

(a) IMRT **(b)** IMPT

Figure 14 – Transverse CT slice for one representative patient. Total dose distributions for the IMRT (a) and IMPT (b) plans with a DE level of 2.3 GyE in the GTV_{SIB} from Jakobi et al. [38]. GTV_{SIB} (green contour), PTV_{all} (blue contour), spinal cord (yellow contour), parotid glands (red contour)

4.3 NTCP models

NTCP models for relevant side effects are used to calculate the NTCP values for the IMRT and IMPT plans and for the combined treatment. The following relevant toxicities are investigated: xerostomia, physician-rated dysphagia, larynx-based and pharyngeal constrictor muscles (PCM)-based aspiration and acute mucositis. They depend on the mean dose $\overline{d}$ (Eq. 5) or the generalized equivalent uniform dose $gEUD$ (Eq. 6) of the considered organ.

$$\overline{d} = \frac{1}{V}\sum_{i}^{V} d_i \tag{5}$$

$$gEUD = \left(\frac{1}{V}\sum_{i}^{V} d_i^{\frac{1}{q}}\right)^{q} \tag{6}$$

- d_i is the dose delivered to the voxel with index i
- V is the set of voxels that belong to the considered organ

- q is the 'volume-effect' parameter [39]. q is smaller than 1. In the special case where $q = 1$, the $gEUD$ is equivalent to the mean dose in the organ.

▶ Xerostomia

Xerostomia describes the dryness in the mouth which may be associated with the lack of saliva production. It occurs when the parotid glands are irradiated, and their function affected. The Lyman-Kutcher-Burman (LKB) model (Eq. 7) [40] describes the probability to get this toxicity as a function of the $gEUD$ of the contralateral parotid gland.

$$NTCP_{LKB} = \phi\left(\frac{gEUD - D_{50}}{D_{50} \cdot m}\right) \tag{7}$$

- ϕ is the cumulative distribution function of the standard normal distribution
- D_{50} is the $gEUD$ given to the whole organ volume that results in 50% complication risk
- m is the slope of the sigmoid curve at D_{50}
- The model parameters are $D_{50} = 39.9$ Gy, $m = 0.4$ and $q = 1$ published by Houweling et al. [28].

▶ Aspiration

Aspiration describes the entry of food, liquid or saliva in the airways. Relevant organs are the PCM and larynx. This toxicity is described by the LKB model (Eq. 7) with the following parameters from Eisbruch et al. [41].

→ For the larynx-based aspiration: $q = 1$, $D_{50} = 46.5$ Gy, $m = 0.5$

→ For the PCM-based aspiration: $q = 0.2$, $D_{50} = 64.5$ Gy, $m = 0.09$

▶ Physician-rated dysphagia

Dysphagia is the difficulty in swallowing. The multimodal model (Eq. 8) describes this toxicity with parameters from Christianen et al. [42].

$$NTCP_{multimodal} = \left(1 + e^{a - b\cdot\overline{d}_1 - c\cdot\overline{d}_2}\right)^{-1} \tag{8}$$

- $\overline{d}_1$ is the mean dose to the superior PCM
- $\overline{d}_2$ is the mean dose to the supraglottic
- The model parameters are $a = 6.09$, $b = 0.057\ \frac{1}{Gy}$, $c = 0.037\ \frac{1}{Gy}$ from Christianen et al. [42]

▶ Acute mucositis

The mucous membranes can be inflamed after irradiation and this can seriously impact the quality of life. The logistic model (Eq. 9) describes this toxicity with parameters from Bhide et al. [43].

$$NTCP_{logisitic} = \left(1 + \left(\frac{D_{50}}{\overline{d}}\right)^{k}\right)^{-1} \tag{9}$$

- $\overline{d}$ is the mean dose to the oral cavity
- The model parameters are $D_{50} = 51$ Gy and $k = 1$ from Bhide et al. [43]

The organs are usually contoured by an experienced physician or dosimetrist. As not all the organs were delineated (because they were located completely in the target volume), the NTCP values depending on these organs couldn't be calculated. The total number of patients for which these OARs are delineated is listed in Table 4.

The contralateral parotid gland and oral cavity are contoured for every patient of the cohort. The NTCP values for xerostomia and acute mucositis can be calculated for every patient. The larynx was not contoured for 3 patients. So, the NTCP values for the larynx-based aspiration can be calculated for 42 HNSCC patients. The PCM is the union of the inferior constrictor muscle, middle constrictor muscle and superior constrictor muscle which were contoured separately. If some patients don't have one of these structures contoured, their NTCP value for the PCM-based aspiration is not calculated. In our case, the PCM was completely delineated for 42 patients. NTCP values for dysphagia can be calculated for 37 patients, because the superior PCM and the supraglottic are not contoured for 2 and 6 different patients, respectively.

Table 4 – Total number of patients for which the NTCP models can be calculated with their corresponding delineated OARs

NTCP models	Delineated OARs	Number of patients (P)
Xerostomia	Contralateral parotid gland	45
Larynx-based aspiration	Larynx	42
PCM-based aspiration	PCM	42
Physician-rated dysphagia	Supraglottic and superior PCM	37
Acute mucositis	Oral cavity	45

5 Rescaled dose distributions and NTCP evaluation

5.1 Rescaling the dose distributions

In this thesis, we rescaled the dose distributions for the original IMRT and IMPT plans obtained from OncoRay such that we obtain two treatment schemes as close as possible to a standard of care, approximately 50-54 GyE in the PTV and 70 GyE in the GTV.

- Simultaneous Integrated Boost = SIB

  The first scheme is a Simultaneous Integrated Boost (SIB). The dose distribution of Phase 2 with DE of 2.6 GyE is rescaled such that 70 GyE are delivered in the GTV_{SIB} and 54 GyE in the PTV_{all} in 30 fractions. This SIB scheme is similar to a standard of care treatment.

- Sequential Boost = SEQ

  The second scheme is a Sequential Boost (SEQ) with a 25-fraction base plan and a 10-fraction boost plan. The original dose distributions of Phase 1 with 2 GyE in the PTV_{all} and Phase 3 with DE level of 2.3 GyE in the GTV_{SIB} are rescaled such that 2 GyE x 25 fractions and 2 GyE x 10 fractions are delivered uniformly in the PTV_{all} and in the GTV-T, respectively. The total doses are 50 GyE in the difference of PTV_{all} and PTV_{adapt} ($PTV_{all} - PTV_{adapt}$), 70GyE in the PTV_{adapt} and 73 GyE in the GTV_{SIB}. Phase 1 delivers a uniform dose to the PTV_{all} and Phase 3 delivers a uniform dose to the PTV_{adapt} with a DE in the $GTV_{SIB,adapt}$. Therefore, when adding Phase 1 and Phase 3 together, an additional dose is present in the PTV_{all} due to dose delivered with Phase 3 to the PTV_{adapt} (Fig. 15). This scheme delivers a sequential boost in the PTV_{adapt} and represents a standard of care treatment.

For the SIB and SEQ scheme, the IMRT and IMPT dose distributions of one transverse CT slice for the representative patient in Figure 14 are shown in Figure 15.

5.2 NTCP evaluation for combined proton-photon radiotherapy

For all IMRT and IMPT treatment plans, a photon and proton dose values per fraction d_i^γ and d_i^p are associated with voxel i. In combined photon-proton radiotherapy with n^p proton fractions and n^γ photon fractions, the cumulative dose $d_i^{combined}$ to voxel i is given by the sum of the photon and proton dose (Eq. 10).

$$d_i^{combined} = n^p \cdot d_i^p + n^\gamma \cdot d_i^\gamma \quad \forall i \tag{10}$$

For a patient j, the mean dose and the $gEUD$ are given by the Equations (11) and (12), where $\overline{d}_j^p$ and $\overline{d}_j^\gamma$ are the proton and photon mean dose per fraction. The number of fractions per treatment (F) equals the sum of the number of photon (n^γ) and proton (n^p) fractions for the SIB scheme (Eq. 13).

$$\overline{d}_j^{combined} = n^p \cdot \overline{d}_j^p + n^\gamma \cdot \overline{d}_j^\gamma \quad \forall j \tag{11}$$

$$gEUD_j^{combined} = \left(\frac{1}{V} \sum_i^V \left(d_i^{combined} \right)^{\frac{1}{q}} \right)^q \quad \forall j \tag{12}$$

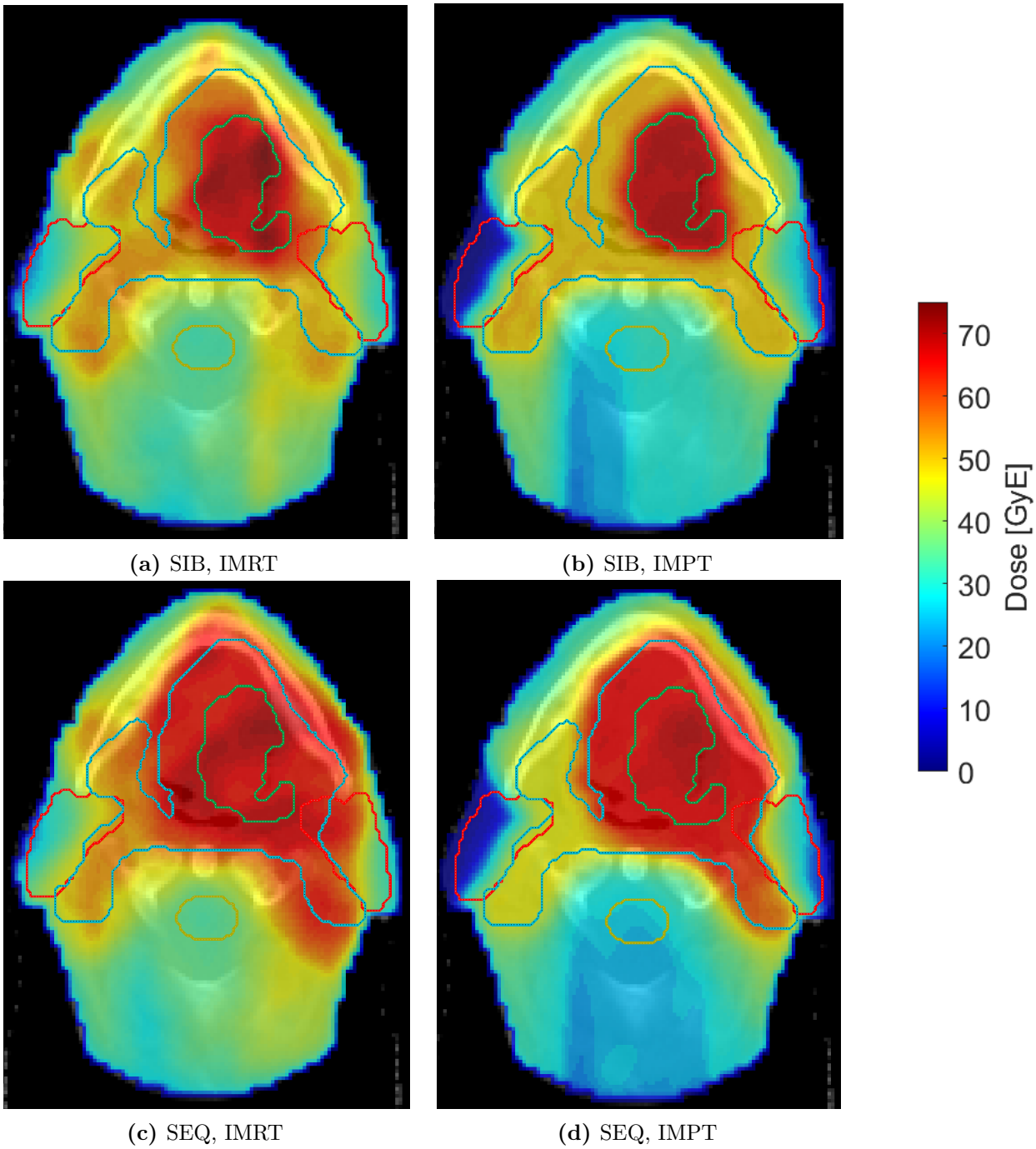

(a) SIB, IMRT **(b)** SIB, IMPT

(c) SEQ, IMRT **(d)** SEQ, IMPT

Figure 15 – Transverse CT slice for the SIB and SEQ cumulative dose distributions for the IMRT (a,c) and IMPT (b,d) plans. GTV_{SIB} (green contour), PTV_{all} (blue contour), spinal cord (yellow contour), parotid glands (red contour)

$$F_j^{SIB} = n_j^{\gamma} + n_j^{p} \quad \forall j \tag{13}$$

For the SEQ scheme, the total proton and photon mean doses are given by the sum of the mean doses in the base and boost plans (Eq. 14). The sum of the number of proton and photon fractions delivered in the base and boost plans is the total number of fractions per treatment for the base and boost plans (Eq. 15).

$$\overline{d_j}^{p} = \overline{d_j}^{p,boost} + \overline{d_j}^{p,base} \qquad \overline{d_j}^{\gamma} = \overline{d_j}^{\gamma,boost} + \overline{d_j}^{\gamma,base} \quad \forall j \tag{14}$$

$$F_{j,base}^{SEQ} = n_j^{\gamma,base} + n_j^{p,base} \qquad F_{j,boost}^{SEQ} = n_j^{\gamma,boost} + n_j^{p,boost} \quad \forall j \tag{15}$$

The NTCP values for combined treatments can be calculated from the NTCP models and the Equations (10), (11), (12) as function of the number of proton fractions n_j^p. For instance, the $NTCP_j$ value for xerostomia (Eq. 7) for a patient j are given by the Equations (16) and (17) for the SIB and SEQ scheme.

$$NTCP_j^{SIB}(n_j^p) = \phi\left(\frac{n_j^p \cdot \overline{d}_j^p + (F^{SIB} - n_j^p) \cdot \overline{d}_j^{\gamma} - D_{50}}{D_{50} \cdot m}\right) \quad \forall j \tag{16}$$

$$NTCP_j^{SEQ}(n_j^{p,base}, n_j^{p,boost}) = \phi\left(\frac{n_j^{p,base} \cdot \overline{d}_j^{p,base} + n_j^{p,boost} \cdot \overline{d}_j^{p,boost}}{D_{50} \cdot m} + \frac{(F_{base}^{SEQ} - n_j^{p,base}) \cdot \overline{d}_j^{\gamma,base} + (F_{boost}^{SEQ} - n_j^{p,boost}) \cdot \overline{d}_j^{\gamma,boost} - D_{50}}{D_{50} \cdot m}\right) \quad \forall j \tag{17}$$

- $\overline{d}_j^{\gamma}$ and $\overline{d}_j^{p}$ are the photon and proton mean dose of the contralateral parotid gland for one fraction
- For the SIB scheme: $F^{SIB} = 30$
- For the SEQ scheme: $F_{base}^{SEQ} = 25$ and $F_{boost}^{SIB} = 10$

For the patient cohort and for each scheme, the average NTCP value ($NTCP_{average}$) is calculated as a function of the number of proton slots that each patient receives (Eq. 18, 19).

$$NTCP_{average}^{SIB} = \frac{1}{P}\sum_{j}^{P} NTCP_j^{SIB}(n_j^p) \tag{18}$$

$$NTCP_{average}^{SEQ} = \frac{1}{P}\sum_{j}^{P} NTCP_j^{SEQ}(n_j^{p,base}, n_j^{p,boost}) \tag{19}$$

- P is the number of patients in the cohort

6 Optimal allocation of proton slots over the given patient cohort

6.1 Method

We assume that, due to limited resources, only a percentage of the total number of fractions can be delivered with protons. As an example, only 20% of all fractions were assumed to be available to treat the 45 HNSCC patients with protons for both schemes (Table 5). A fraction-wise selection strategy and a patient-wise selection strategy are developed to optimally allocate the number of proton slots available (N_{avail}) over the patient cohort with the goal of minimizing the average number of expected complications ($NTCP_{average}$). The methodology for these strategies is detailed in the sections 6.1.1 and 6.1.2. The $NTCP_{average}$ values (Eq. 18, 19) are used to evaluate the benefit of combined proton-photon therapy at a population level.

Table 5 – Number of fractions for the SIB and SEQ schemes to treat all the patients. N_{tot} = total number of fractions, N_{avail} = number of proton fractions available

	20% of all fractions	All fractions required
SIB	$N_{avail}^{SIB} = 270$	$N_{tot}^{SIB} = 1350$
SEQ	$N_{avail}^{SEQ} = 315$	$N_{tot}^{SEQ} = 1575$

The methodology is applied for a range of limited proton fractions ($N_{avail} \in \{0, ..., N_{tot}\}$).

6.1.1 Fraction-wise selection

The fraction-wise selection strategy assigns the limited number of proton fractions to the patients who benefit the most on a fractional basis. In this strategy, we investigate three methodologies in which some fractions are delivered with protons and the rest with photons. In that case, the patients receive a combined proton-photon treatment. Three algorithms were developed to determine the optimal number of proton fractions per patient that minimizes the total number of expected complications over the patient cohort: a continuous optimization algorithm, a linear integer optimization algorithm and a greedy heuristic algorithm. All the algorithms find the number of proton fractions for each patient that minimizes the $NTCP_{average}$ value of the patient cohort. They are subject the two following constraints:

- The number of proton fractions is bounded between 0 and 30.
- The sum of the number of proton fractions delivered to each patient must equal the number of proton fractions available.

a) Continuous optimization algorithm

The continuous optimization algorithm (Eq. 20) assumes the number of proton fractions (n_j^p) to be continuous. It is subject to the constraints (21) and (22).

Formally, the optimization problem for the SIB scheme is stated as:

$$\underset{n_j^p}{\text{minimize}} \qquad \frac{1}{P}\sum_{j}^{P} NTCP_j^{SIB}(n_j^p) \tag{20}$$

$$\text{subject to} \qquad 0 < n_j^p < F_j^{SIB} \quad \forall\ j \tag{21}$$

$$\sum_{j}^{P} n_j^p = N_{avail}^{SIB} \tag{22}$$

The final number of proton fractions is rounded. The Matlab function *fmincon* is used to find the minimum of the constrained and nonlinear function (Eq. 20).

b) Linear integer optimization algorithm

As the number of proton slots are integers, a linear integer programming algorithm is applied to implement the fraction-wise selection strategy. This algorithm is detailed for the SIB scheme (Eq. 23) and SEQ scheme (Eq. 26).

For the SIB scheme, the $NTCP_{kj}^{SIB}$ is the NTCP value for patient j receiving k proton fractions. Each $NTCP_{kj}^{SIB}$ is associated with a binary variable $x_{kj} \in \{0, 1\}$. $x_{kj} = 1$, if patient j receives k proton fractions. $x_{kj} = 0$, if patient j does not receive exactly k proton fractions. The sum of x_{kj} for a patient j over the number of proton fractions k equals 1 (Eq. 24). The sum over proton fractions delivered to each patient must equal the number of proton fractions available N_{avail}^{SIB} (Eq. 25).

$$\underset{x_{kj}}{\text{minimize}} \qquad \frac{1}{P}\sum_{j}^{P} NTCP_{kj}^{SIB} \cdot x_{kj} \tag{23}$$

$$\text{subject to} \qquad \sum_{k}^{F^{SIB}} x_{kj} = 1 \quad \forall\ j \tag{24}$$

$$\sum_{k}^{F^{SIB}} \sum_{j}^{P} k \cdot x_{kj} = N_{avail}^{SIB} \tag{25}$$

- $x_{kj} \in \{0, 1\}$
- $k \in \{0, 1, ..., F_j^{SIB}\}$ with $F_j^{SIB} = 30$

For the SEQ scheme, the $NTCP_{\alpha\beta j}^{SEQ}$ is the NTCP value for patient j receiving α proton fractions with the base plan and β proton fractions with the boost plan. Each $NTCP_{\alpha\beta j}^{SEQ}$ is associated to a $x_{\alpha\beta j}$ value. $x_{\alpha\beta j} = 1$, if patient j receives α and β proton fractions. $x_{\alpha\beta j}$ = 0, if patient j does not receive exactly α and β proton fractions (Eq. 27). The sum over proton fractions in the base plan and proton fractions in the boost plan must equal the number of proton fractions available N_{lim}^{SEQ} (Eq. 28).

$$\underset{x_{\alpha\beta j}}{\text{minimize}} \qquad \frac{1}{P}\sum_{j}^{P} NTCP_{\alpha\beta j}^{SEQ} \cdot x_{\alpha\beta j} \tag{26}$$

$$\text{subject to} \qquad \sum_{\alpha}^{F_{base}^{SEQ}} \sum_{\beta}^{F_{boost}^{SEQ}} x_{\alpha\beta j} = 1 \quad \forall\ j \tag{27}$$

$$\sum_{\alpha}^{F_{base}^{SEQ}} \sum_{\beta}^{F_{boost}^{SEQ}} \sum_{j}^{P} (\alpha+\beta) \cdot x_{\alpha\beta j} = N_{avail}^{SEQ} \tag{28}$$

- $x_{\alpha\beta j} \in \{0,1\}$
- $\alpha \in \{0,1,...,F_{j,base}^{SEQ}\}$ and $\beta \in \{0,1,...,F_{j,boost}^{SEQ}\}$ with $F_{j,base}^{SEQ} = 25$, $F_{j,boost}^{SEQ} = 10$

The Matlab function *intlinprog* is used to find the minimum of these linear and integer problems.

c) Greedy heuristic algorithm

The greedy heuristic algorithm assigns proton slots iteratively to the patients who benefit the most from one additional proton fraction. This algorithm is detailed for the SIB scheme and SEQ scheme.

For the SIB scheme, the $\Delta NTCP_{kj}$ (Eq. 29) is the NTCP improvement for a patient j receiving one more proton fraction k.

$$\Delta NTCP_{kj} = NTCP_{(k-1)j} - NTCP_{kj} \quad \text{with} \quad k \in \{1,2,\ldots,F_j^{SIB}\} \tag{29}$$

In each iteration, the algorithm finds the highest $\Delta NTCP_{kj}$ over the patient cohort and the patient with the highest $\Delta NTCP_{kj}$ is assigned one more proton fraction. This is repeated for N_{avail}^{SIB} iterations.

For the SEQ scheme, the proton fraction can be assigned to either the base or the boost plan. The $\Delta NTCP_{\alpha(\beta-1)j}$ (Eq. 30) and $\Delta NTCP_{(\alpha-1)\beta j}$ (Eq. 31) are the NTCP improvements for a patient j receiving one more proton fraction α or β. This algorithm finds the highest $\Delta NTCP_{\alpha(\beta-1)j}$ or $\Delta NTCP_{(\alpha-1)\beta j}$ over the patient cohort. Patient j with the highest $\Delta NTCP_{\alpha(\beta-1)j}$ or $\Delta NTCP_{(\alpha-1)\beta j}$ receives one more proton fractions.

$$\Delta NTCP_{\alpha(\beta-1)j} = NTCP_{(\alpha-1)(\beta-1)j} - NTCP_{\alpha(\beta-1)j} \tag{30}$$

$$\Delta NTCP_{(\alpha-1)\beta j} = NTCP_{(\alpha-1)(\beta-1)j} - NTCP_{(\alpha-1)\beta j} \tag{31}$$

$$\text{with} \quad \alpha \in \{1,2,...,F_{j,base}^{SEQ}\} \quad \text{and} \quad \beta \in \{1,2,...,F_{j,boost}^{SEQ}\}$$

- The continuous optimization algorithm would yield the optimal solution if the proton slots were not integer variables. The rounding at the end of this algorithm does not guarantee to obtain an optimal allocation.
- The linear integer optimization algorithm guarantees to find the optimal solution as it tests every possible allocation and finds the one that minimizes the $NTCP_{average}$ value.
- The greedy heuristic algorithm could potentially find the local minimum and is expected to get the same allocation as the linear integer optimization algorithm if the NTCP values for proton and photons are located on the convex part of the NTCP curve for all considered patients.

6.1.2 Patient wise-selection

For the patient-wise selection strategy, single-modality treatments are considered. Patients are assigned either to proton or photon therapy for the whole treatment based on the NTCP values for IMRT ($NTCP^{IMRT}$) and IMPT ($NTCP^{IMPT}$). In this algorithm, the number of proton fractions available (N_{avail}) must be a multiple of the number of fractions per treatment F (Eq. 32).

$$N_{avail}^{SIB} = m \cdot F^{SIB} \text{ and } N_{avail}^{SEQ} = m \cdot \left(F_{base}^{SEQ} + F_{boost}^{SEQ}\right) \text{ with } m \in \mathbb{N} \tag{32}$$

The $\Delta NTCP_j$ (Eq. 33) is calculated for every patient j. Patients with the highest $\Delta NTCP$ are assigned to pure IMPT until the number of proton slots is depleted. The rest of the patients receive pure IMRT.

$$\Delta NTCP_j = NTCP_j^{IMRT} - NTCP_j^{IMPT} \tag{33}$$

6.2 Results

6.2.1 NTCP values for the SIB and SEQ schemes

For the 45 HNSCC patients, the doses in the contralateral parotid gland are obtained from the IMRT and IMPT plans for the SIB and SEQ schemes (Annex A). From these doses, the NTCP values for xerostomia (Eq. 7) are calculated for all the patients for both schemes (Fig. 16). The ΔNTCP values (Eq. 4) for xerostomia for the SIB scheme are shown in Figure 17. The patients are ordered according to their $\Delta NTCP$ values for the SIB scheme.

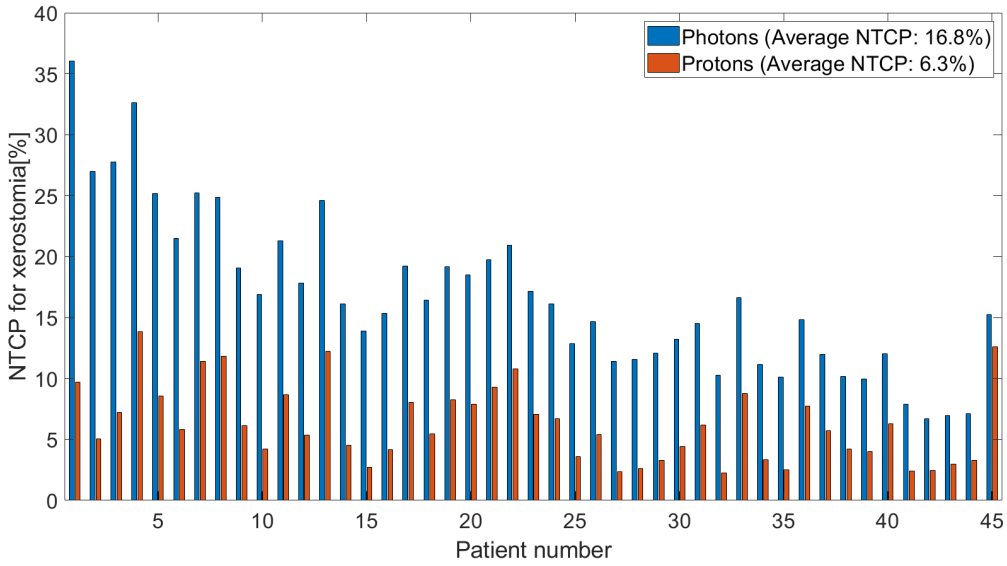

(a) SIB scheme

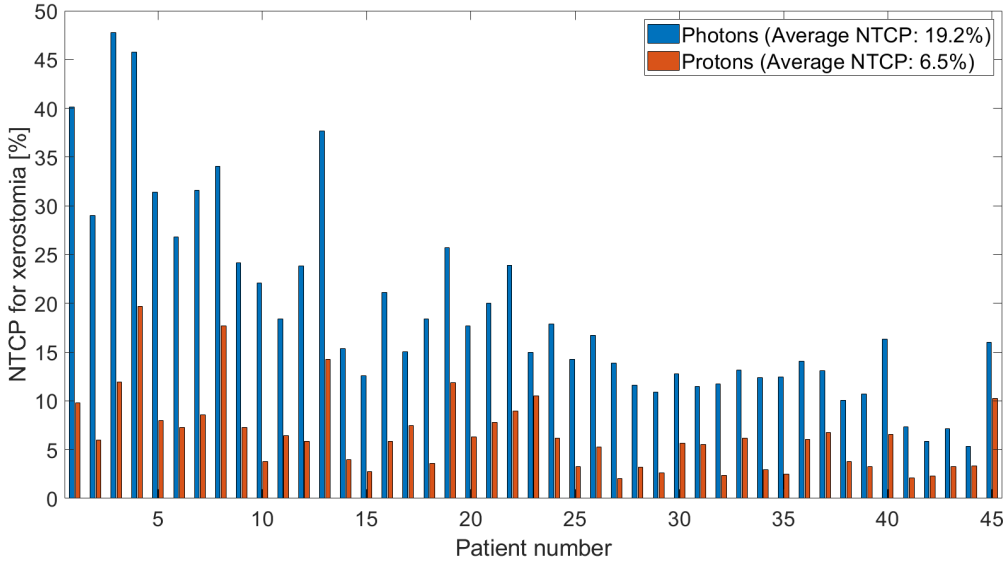

(b) SEQ scheme

Figure 16 – The NTCP values for xerostomia for the 45 HNSCC patients for the IMRT (blue) and IMPT (red) plans for the SIB (a) and SEQ (b) schemes

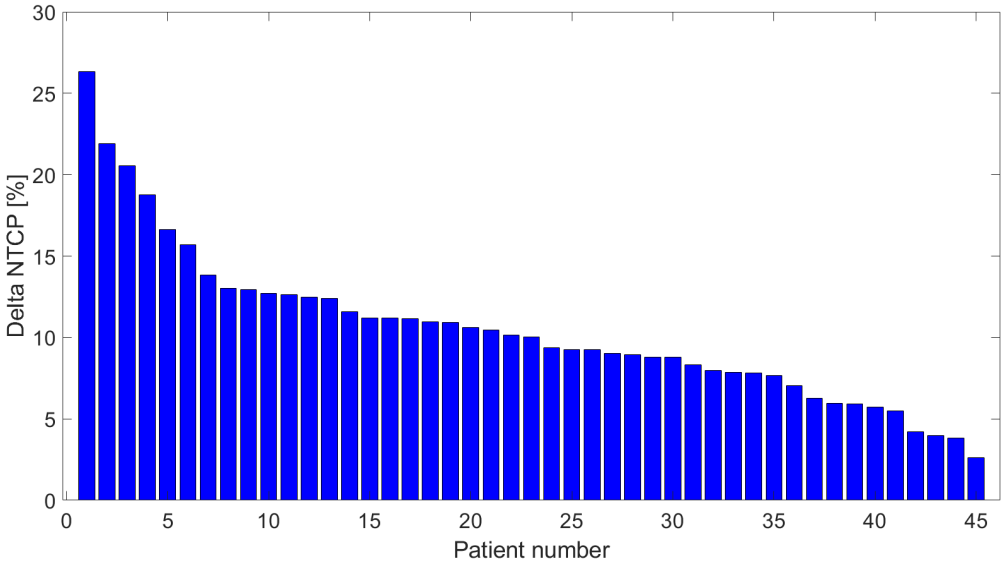

Figure 17 – The ΔNTCP values for xerostomia for the 45 HNSCC patients for the the SIB scheme

The boxplots for the NTCP values for photons and protons are obtained for xerostomia (Fig. 18). Boxplots for the other toxicities (dysphagia, larynx- and PCM-based aspiration, acute mucositis) are shown in Annex B for the SIB and SEQ schemes.

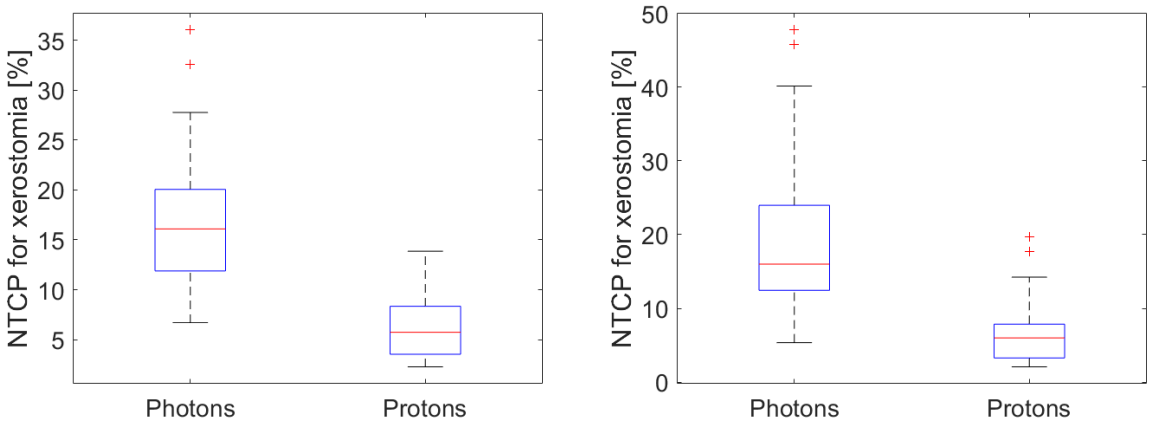

(a) SIB scheme **(b)** SEQ scheme

Figure 18 – The boxplots for the NTCP values for xerostomia for photons and protons for the SIB (a) and SEQ (b) schemes for the 45 HNSCC patients

IMPT reduces the NTCP values for xerostomia over IMRT for all 45 HNSCC patients for the SIB and SEQ schemes (Fig. 16, 18). If all the patients are treated with IMPT compared to IMRT, a decrease in $NTCP_{average}$ value (Eq. 18) for xerostomia of 10.5% for the SIB scheme and 12.7% for the SEQ scheme is feasible (Table 6). The $\Delta NTCP$ value varies for each patient from 2% to 26% for the SIB scheme (Fig. 17) and from 2% to 35% for the SEQ scheme (Fig. 16b).

6.2.2 Optimal allocations for 20% of proton slots available

20% of proton slots available are optimally allocated over the 45 HNSCC patients based on the NTCP model for xerostomia for the SIB and SEQ schemes (Fig. 19, 20). These optimal allocations are obtained for the fraction-wise and the patient-wise selection strategies (sections 4.1.1 and 4.1.2).

The linear integer optimization algorithm is used for the fraction-wise selection as it yields to the optimal allocation of limited proton slots. Other algorithms (continuous optimization, greedy heuristic) were also investigated and near identical results were obtained.

a) SIB scheme: $N_{avail}^{SIB} = 270$ proton slots

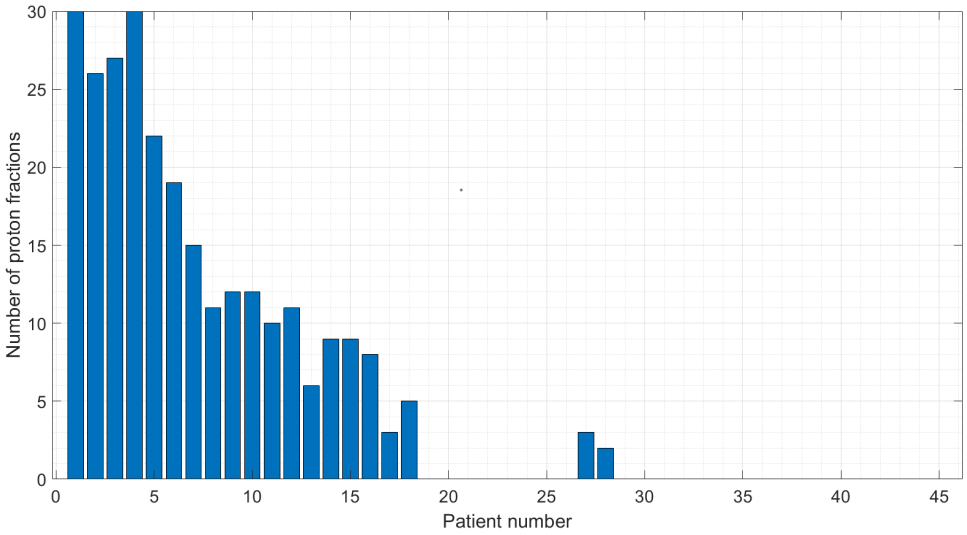

(a) Fraction-wise selection

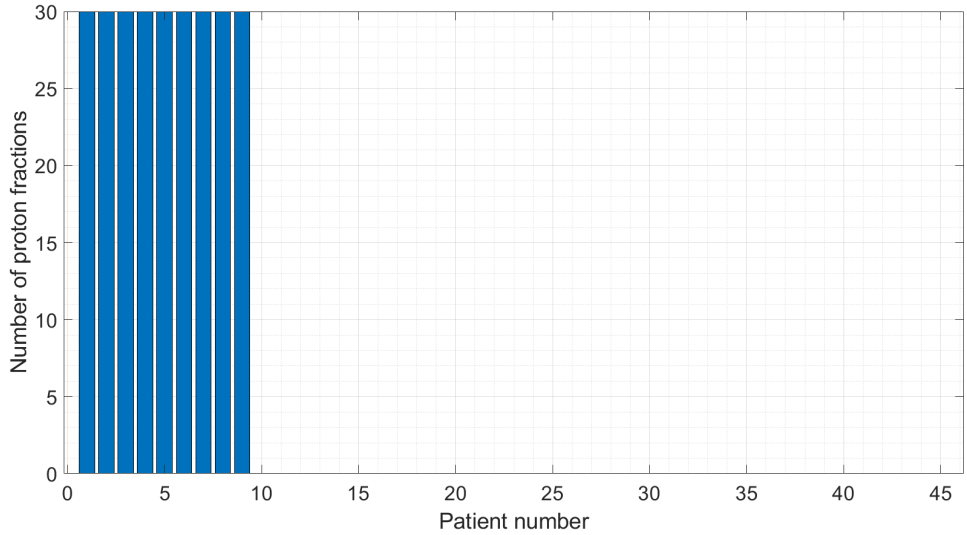

(b) Patient-wise selection

Figure 19 – The optimal allocation of 270 proton fractions among the 45 HNSCC patients for the fraction-wise (a) and patient-wise (b) selection for the SIB scheme based on the NTCP model for xerostomia

For the fraction-wise selection (Fig. 19a), 2 patients receive only proton fractions and 25 patients receive only photons. 18 patients receive a combined proton-photon treatment. The patients with the highest $\Delta NTCP$ value (Fig. 17) receive the largest number of proton fractions (Fig. 19a). The number of fractions per patient depends also on the absolute NTCP values. For instance, patient 4 receives a higher number of proton fractions but has a lower ΔNTCP compared to patients 2 and 3 (Fig. 19a). In that case patient 4 has higher $NTCP^{IMRT}$ and $NTCP^{IMPT}$ values compared to patients 2 and 3 (Fig. 16a).

For the patient-wise selection (Fig. 19b), the first 9 patients are assigned to pure IMPT because they have the highest $\Delta NTCP$ values among the patient cohort. The 36 other patients are assigned to pure IMRT.

b) SEQ scheme: $N_{aval}^{SEQ} = 315$ proton slots

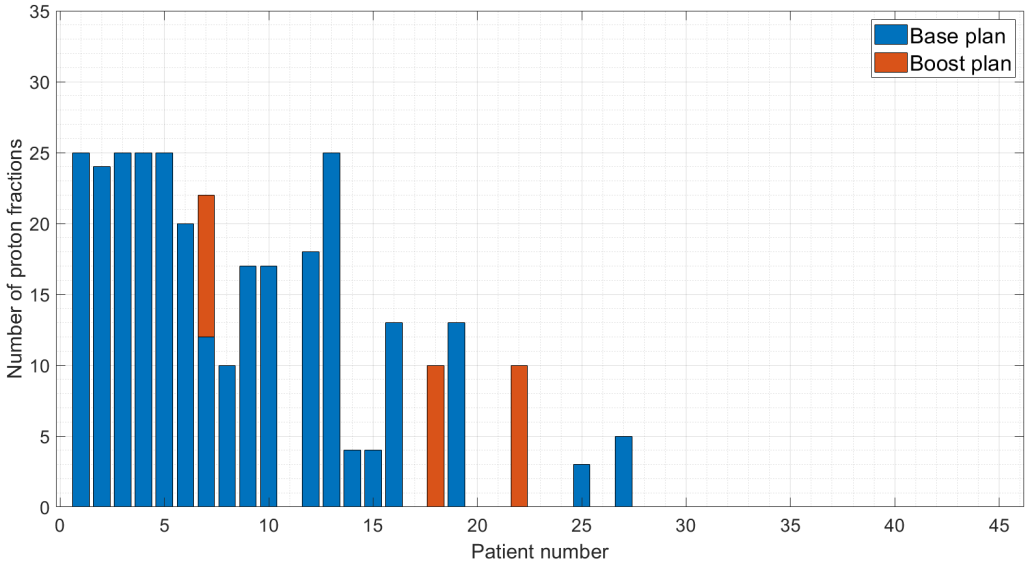

(a) Fraction-wise selection

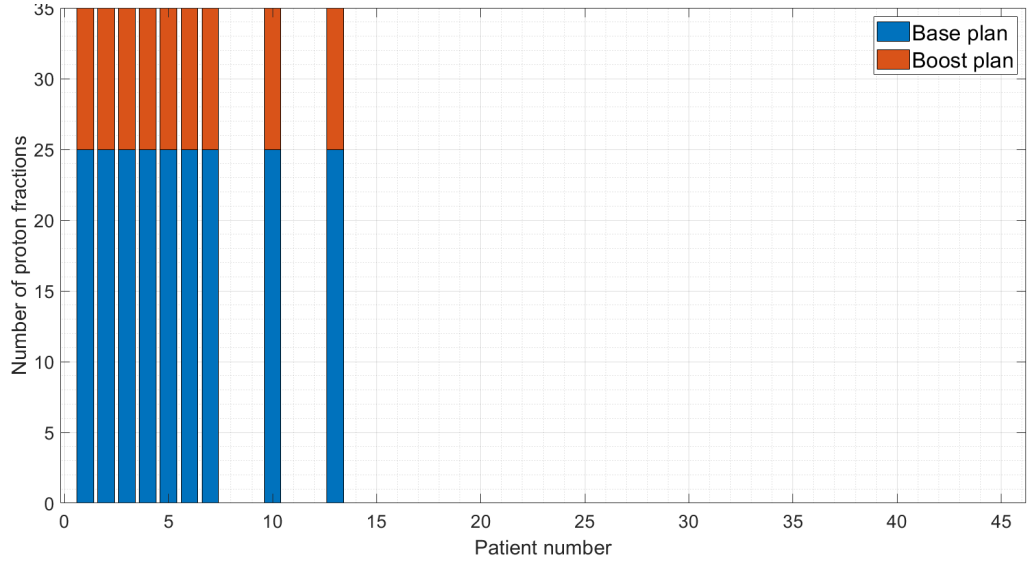

(b) Patient-wise selection

Figure 20 – The optimal allocation of 315 proton fractions among the 45 HNSCC patients for the fraction-wise (a) and patient-wise (b) selection for the SEQ scheme based on the NTCP model for xerostomia

For the fraction-wise selection (Fig. 20a), 20 patients receive a combined proton-photon treatment and 25 patients receive only photons. For the 20 patients treated with a combined treatment, only 3 patients receive proton slots for the boost plan whereas most proton slots are used for base plans. The Δdose per fraction in Figure 21 represents the decrease of mean dose by delivering one proton fraction instead of one photon fraction. Figure 21 shows the Δdose in the contralateral parotid gland for the SEQ scheme for the base and boost plans. Patients 7, 18 and 22 receive some proton fractions in the boost plan as they have a higher Δdose per fraction for the boost than the base plan, corresponding to higher ΔNTCP value (Fig. 16b).

For the patient-wise selection (Fig. 20b), the first 7 patients and the patients number 10 and 13 receive a complete IMPT treatment because they have the highest $\Delta NTCP$ values for the SEQ scheme. The 36 other patients are assigned to pure IMRT.

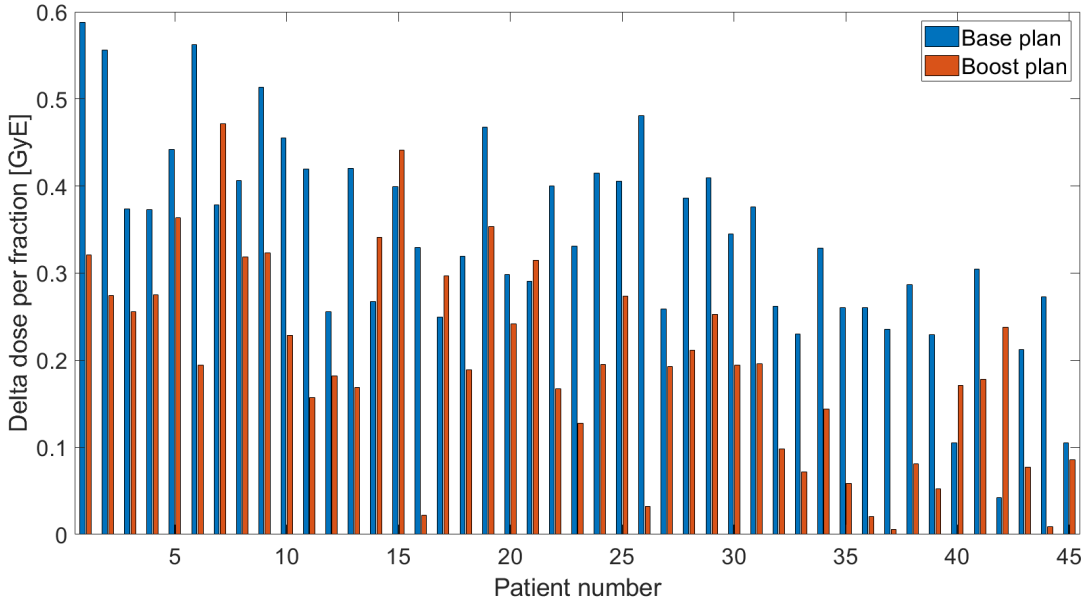

Figure 21 – The Δdose per fraction to the contralateral parotid gland for the base and boost plans of the SEQ scheme for the 45 HNSCC patient

c) The $NTCP_{average}$ values for 20% of proton slots available

The $NTCP_{average}$ values for xerostomia for the SIB and SEQ schemes (Eq. 18, 19) are calculated for the patient-wise and fraction-wise selection strategies with 20% of proton slots available. The $NTCP_{average}$ values are shown in Table 6 for the situation where all the patients are treated with only IMRT, only IMPT and the two strategies with limited proton resources.

Table 6 – $NTCP_{average}$ values for 45 HNSCC patients treated with pure IMRT or IMPT and with 20% of proton slots available for a patient-wise or fraction-wise selection

	All patients treated with IMRT	Patient-wise selection (20% of proton slots)	Fraction-wise selection (20% of proton slots)	All patients treated with IMPT
SIB	16.8%	13.2%	13.0%	6.3%
SEQ	19.2%	14.2%	13.6%	6.5%

The optimal allocation of proton slots for the situation where 20% of all fractions are delivered with protons are illustrated for the SIB scheme (Fig. 19) and the SEQ scheme (Fig. 20). With 20% of proton slots available, the benefit in terms of $NTCP_{average}$ for xerostomia is 0.2% (SIB scheme) and 0.6% (SEQ scheme) for the fraction-wise selection over the patient-wise selection.

6.2.3 The $NTCP_{average}$ values for a range of proton slots available

Based on the NTCP model for xerostomia, the optimal allocation for a range of proton slots available (from 0 to N_{tot}) are obtained for the fraction-wise and patient-wise selection strategies for the SIB and SEQ schemes. From these allocations, the $NTCP_{average}$ values for xerostomia are calculated as function of the number of proton slots available (Fig. 22).

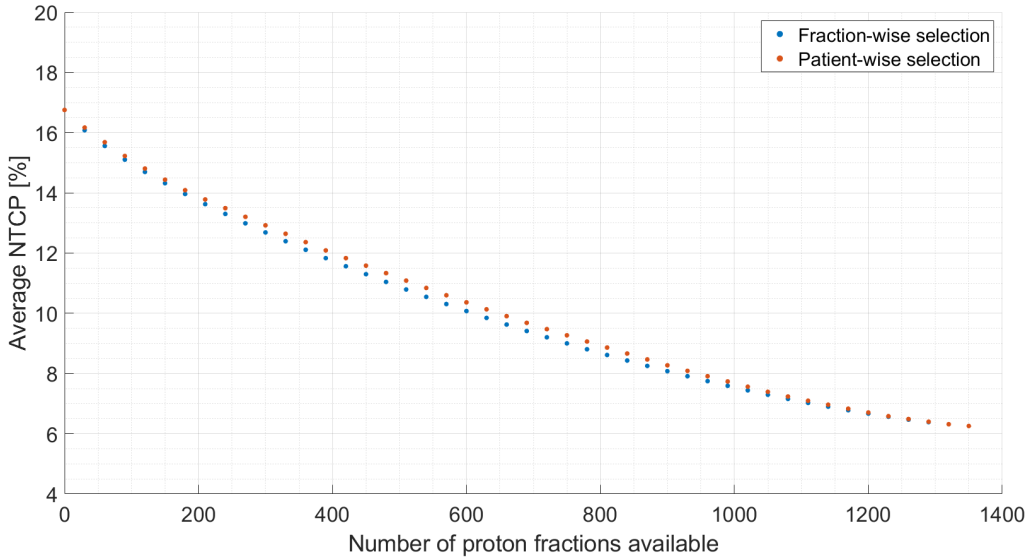

(a) SIB scheme

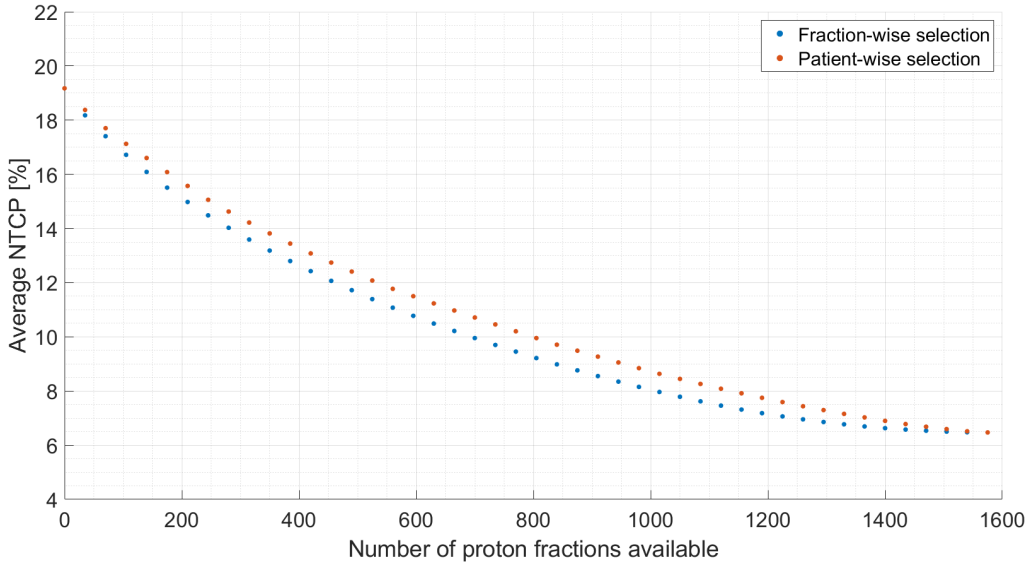

(b) SEQ scheme

Figure 22 – The $NTCP_{average}$ values for xerostomia for the fraction-wise (blue points) and patient-wise (red points) selection strategies as function of the number of proton fractions available N_{avail} for the SIB (a) and SEQ (b) scheme

The small benefit of the fraction-wise selection for the SIB scheme is also observed for a range of proton slots available (Fig. 22a). The improvement of $NTCP_{average}$ value can be explained by the fact that the first proton fractions delivered to the patients are the most beneficial since all patients are located on the convex part of the NTCP curve. However, this benefit is small as the difference in proton and photon mean doses are small enough for the NTCP curve to be approximately linear over the small range of mean doses. A larger benefit is observed for the SEQ scheme, where combined treatments can exploit the fact that some patients benefit from proton boost plans and others from proton base plans (Fig. 22b). The $NTCP_{average}$ values for dysphagia, acute mucositis, larynx-based and PCM-based aspiration for a range of proton slots available are also obtained for the SIB and SEQ schemes and shown in Annex D. For the SEQ scheme, similar results are obtained for dysphagia, acute mucositis, larynx-based and PCM-based aspiration. However, for the SIB scheme and for these toxicities, no benefit of a fraction-wise over a patient-wise selection can be observed.

6.3 Comments

1. For the SEQ scheme, the NTCP values for PCM-based aspiration, larynx-based aspiration and dysphagia are up to 25% higher than for the SIB scheme (Annex D). These toxicities depend on the doses delivered in the larynx and the PCM which are higher for the SEQ scheme than the SIB scheme. The dose distributions for a sagittal CT slice for patient number 5 are illustrated for IMRT and IMPT for both schemes in Figure 23. For this patient, the doses in the larynx and the PCM are up to 10 GyE higher in the neighbourhood of the GTV_{SIB} for the SEQ scheme than the SIB scheme. This is due to the differences in the definition of the boost target volume, which includes only the GTV for the SIB scheme and a substantial margin around the GTV for the SEQ scheme.

2. The patients who benefit from proton slots are not the same depending on the considered NTCP model. The optimal allocations for 20% of proton slots available based on the NTCP model for acute mucositis are illustrated in Annex C. For the SIB scheme, patient 14 is the only patient who receives proton fractions with the allocation based on both the NTCP model for xerostomia (19a) and the NTCP model for oral mucositis. For this scheme, the allocations based on the NTCP model for acute mucositis are the same for the fraction-wise and patient-wise selection. The patient cohort has no benefit of combined treatment if the proton slots allocation is based on the NTCP model for acute mucositis.

3. The number of proton fractions to achieve a given $NTCP_{average}$ can be reduced with a fraction-wise selection compared to a patient-wise selection. For instance, to achieve an average NTCP of 14.2%, combined treatment would require only 265 (16.8%) proton fractions instead of 315 (20%) for the SEQ scheme (Table 7).

Table 7 – Number (and percentage) of proton fractions to achieve an equivalent $NTCP_{average}$ with a patient-wise and fraction-wise selection for the SEQ scheme

$NTCP_{average}$	Patient-wise selection	Fraction-wise selection
14.2%	315 (20%)	265 (17%)
10.0%	805 (51%)	700 (44%)

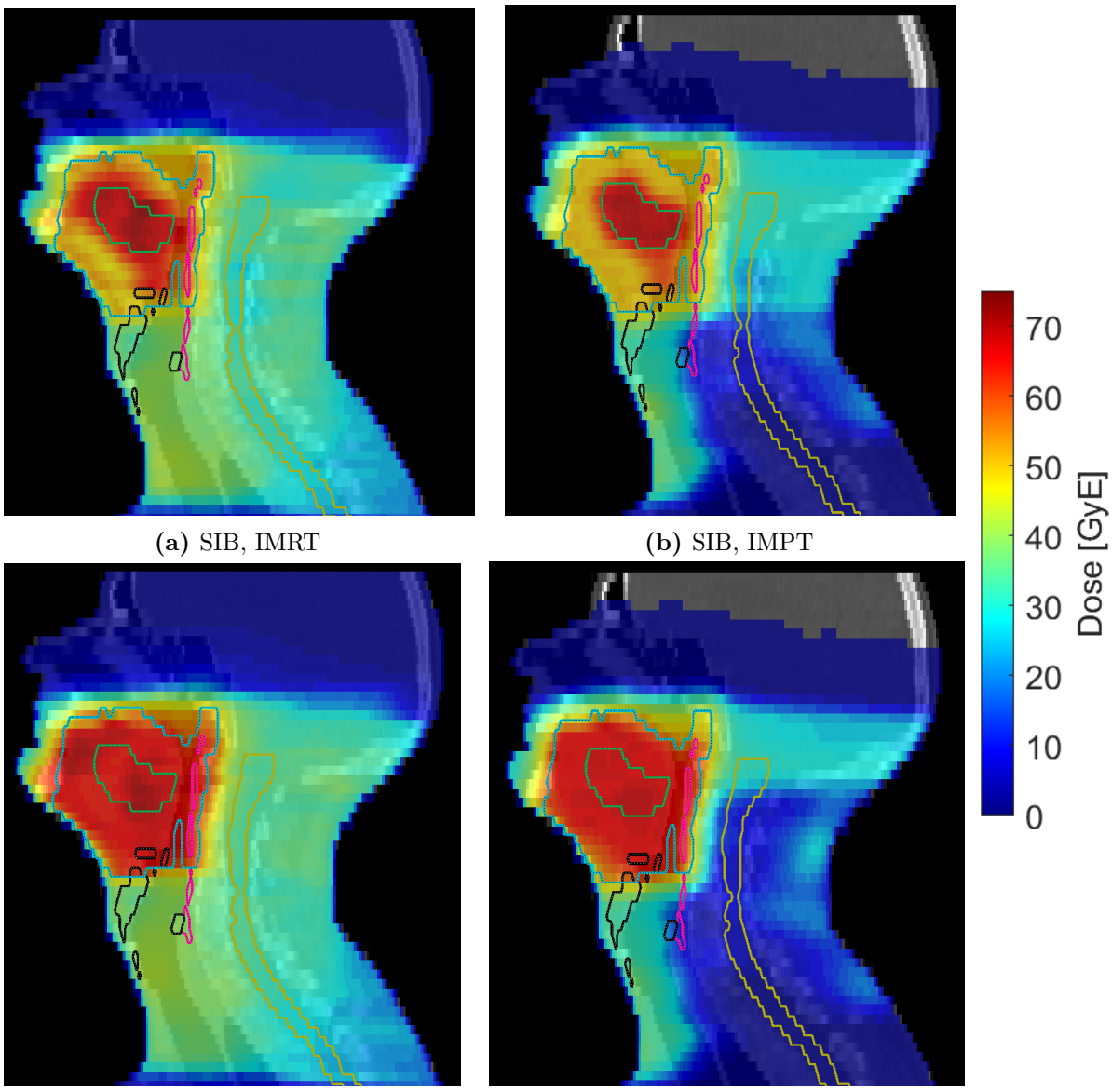

(a) SIB, IMRT **(b)** SIB, IMPT

(c) SEQ, IMRT **(d)** SEQ, IMPT

Figure 23 – Sagittal CT slice of the cumulative dose distributions for the IMRT and IMPT plans for the SIB (a,b) and SEQ (c,d) schemes. GTV_{SIB} (green contour), PTV_{all} (blue contour), spinal cord (yellow contour), larynx (black contour), PCM (rose contour)

7 Maximizing the benefit of combined proton-photon radiotherapy for the continuous operation of a clinic over time

We consider a clinic offering both photons and protons and a scenario, in which only limited PT slots are available per day for treating HNSCC patients with the SIB scheme. In chapter 6, we considered an idealized scenario in which all the 45 HNSCC patients were known at the time of distributing the proton slots. However, in reality, new patients may come every day in the clinic. So, we develop an algorithm which simulates a clinic distributing optimally the proton and photon slots to HNSCC patients over time. In order to simulate a radiotherapy clinic over a long period of time, a larger cohort is obtained by generating random patients to create this situation in section 7.1.1. We design a daily slot allocation strategy in which proton slots are allocated on a daily basis to patients currently under treatment who benefit the most from one proton fraction. In section 7.1.2, we compare this strategy to a threshold-based patient selection in which patients are either allocated to IMRT or IMPT for the entire treatment. The scenarios are based on the NTCP model for xerostomia. In section 7.1.3, the criteria to simulate this situation is detail, in which patients come and are treated in the clinic. Finally, the average NTCP values are calculated to evaluate the benefit of combined proton-photon radiotherapy over the threshold-based patient selection.

7.1 Method

7.1.1 Generate random patients

To increase the size of the patient cohort, the mean doses in the contralateral parotid gland are sampled from a 2D gaussian distribution function (Eq. 34) derived from the doses of the 45 HNSCC patients.

$$y(x) = \frac{1}{\sqrt{|\sum|(2\pi)^2}} e^{-\frac{1}{2}(x-\mu)\sum^{-1}(x-\mu)} \tag{34}$$

- $\mu = \begin{bmatrix} \overline{d}^{\gamma} \\ \overline{d}^{p} \end{bmatrix}$ is a vector with $\overline{d}^{\gamma} = \frac{1}{P}\sum_j^P d_j^{\gamma}$ and $\overline{d}^{p} = \frac{1}{P}\sum_j^P d_j^{p}$, i.e. the average proton and photon mean dose in the contralateral parotid gland for the 45 HNSCC patients
- $\sum = \begin{bmatrix} \sigma_{\gamma}^2 & \sigma_{\gamma}\sigma_p \\ \sigma_{\gamma}\sigma_p & \sigma_p^2 \end{bmatrix}$ is the covariance matrix with $\sigma_{\gamma}^2 = \frac{1}{P}\sum_j^P (d_j^{\gamma} - \overline{d}^{\gamma})^2$, $\sigma_p^2 = \frac{1}{P}\sum_j^P (d_j^{p} - \overline{d}^{p})^2$, $\sigma_p\sigma_{\gamma} = \frac{1}{P}\sum_j^P (d_j^{p} - \overline{d}^{p})(d_j^{\gamma} - \overline{d}^{\gamma})$ the variances for photon and proton for the 45 HNSCC patients

The Matlab function *mnvrnd* is used to generate the random mean doses for new HNSCC patients.

7.1.2 Allocation scenarios

Two allocation scenarios to allocate the proton slots are presented. We assume a constant number of proton slots per day (N_{day}).

a) Daily slot allocation strategy

We assume a clinic offering both proton and photon therapy and is operational 5 days per week (e.g. the University Hospital Carl Gustav Carus in Dresden). The daily slot allocation strategy allows for combined treatment and is inspired from the greedy heuristic algorithm described in section 6.1.1. This strategy selects, on a daily basis, the patients currently under treatment (P_{clinic}) who benefit the most from a proton fraction on the respective day.

To calculate the $\Delta NTCP_{kj}$ value (Eq. 29) of all patients currently under treatment, the number of proton and photon fractions that the patients already receive are taken into account and all future fractions are assumed to be delivered with photon fractions. As an example, we consider a patient p in the clinic who received 5 proton fractions and 3 photon fractions so far. The remaining fractions (22) are assumed to be deliver with photon fractions. To determinate if the patient p will receive a proton or a photon fraction, we compare the NTCP values for a treatment with 5 proton fractions and 25 photon fractions ($NTCP_{5p}$) and a treatment with 6 proton fractions and 24 photon fractions ($NTCP_{6p}$). The $\Delta NTCP_{6p}$ (Eq. 35) value is the improvement by distributing one more proton slot instead of one photon slot to patient p.

$$\Delta NTCP_{6p} = NTCP_{5p} - NTCP_{6p} \tag{35}$$

We compare the $\Delta NTCP_{6p}$ value for the patient p with all $\Delta NTCP_{kj}$ values of the patients under treatment. The proton slots available per day (N_{day}) are assigned to the patients with the highest $\Delta NTCP_{kj}$. The remaining patients on that day receive a photon fraction. In this scenario, proton slots are reassigned daily to patients currently under treatments who benefit the most.

b) Threshold-based patient selection

The threshold-based patient selection assigns the patient to IMPT for the whole treatment if the following conditions hold:

- The $\Delta NTCP_j$ (Eq. 33) of the incoming patient j exceeds a $\Delta NTCP_{threshold}$ (e.g. 5%, 10%, 15%):
$$\Delta NTCP_j \geq \Delta NTCP_{threshold}$$
- A proton slot is available the day the patient arrives

In this scenario, the patients start their treatment the day they arrive. Once they are assigned to IMPT, the proton slots are blocked for the next 30 days. If the two conditions are not fulfilled, the patients are assigned to IMRT.

7.1.3 Criteria to simulate a clinical situation

Based on the SIB scheme, the NTCP model for xerostomia and the previous scenarios, a simulation of HNC patients treatment over time is realized with the following assumptions:

i. 2 new HNSCC patients come in the clinic per week on average, corresponding to approximately 100 patients per year. This approximation corresponds to the number of new HNSCC cases from the University Hospital of Zürich for one year.

ii. The patients complete the treatment when receiving 30 fractions ($F_j^{SIB} = 30$) after 6 weeks. On average, 12 patients would be under treatment per week.

iii. To treat all the HNSCC patients with protons, 12 proton slots per day would be needed. We assume limited proton resources, e.g. 3 proton slots per day are available for HNSCC patients, and a larger number of photon fractions than proton fractions

For the presented results, the simulation is carried out for a period of 12'000 days. The main steps of the simulation are the following:

1. We randomly decides if a new HNSCC patient comes in the clinic on every day with a threshold of 0.4 corresponding to the assumption that there is 2 new HNSCC patients on average per week.

2. If yes, the proton and photon mean doses for this patient are randomly drown from the 2D Gaussian distribution. The new patient is considered to be under treatment from now on.

3. – For the daily slot allocation strategy, the $\Delta NTCP_{kj}$ values are calculated for all patients on every day. The proton slots available are distributed to the patients with the highest $\Delta NTCP_{kj}$ values.
   – For the threshold-based patient selection, $\Delta NTCP_j$ value for the new patient is calculated and this patient is assigned to pure IMPT if the two conditions are fulfilled (see section 7.1.2 b)).

Once the simulation is performed, the $NTCP_{average}$ (Eq. 18) is calculated from the final allocation of proton slots of all the patients for 11'200 days. To avoid any issues with the initial and ending conditions, the first and last 400 days are not considered in the final computation of the $NTCP_{average}$. The number of days was chosen to be large enough to minimize the fluctuation on the final $NTCP_{average}$ value due to the randomness of the process. The simulation is performed many times with the goals to:

a) Find the optimal $NTCP_{threshold}$ for the threshold-based patient selection with 3 proton slots per day ($N_{day} = 30$). The simulation was performed with $NTCP_{threshold}$ varying from 0% to 25% with an increment of 1%;

b) Investigate the allocation of proton slots over a cohort of 100 HNSCC patients for the model-based patient selection (with $NTCP_{threshold} = 10\%$) and the daily slot allocation with 3 proton slots per day;

c) Estimate the benefit of the daily slot allocation over the threshold-based patient selection (with $NTCP_{threshold} = 10\%$) as function of the number of proton slots per day (N_{day}) from 1 to 10.

7.2 Results

7.2.1 Sample mean doses to the contralateral parotid gland

The mean doses to the contralateral parotid gland for photon and proton are sampled from the 2D gaussian distribution (Eq. 34) derived from contralateral parotid gland doses of 45 HNSCC patients for the SIB scheme. 100 samples which represent simulated new HNSCC patients for one year are illustrated in Figure 24. Their corresponding $\Delta NTCP$ value is calculated. Half of the 100 samples have a $\Delta NTCP$ value higher than 10%. If a sample is above the red line, the $\Delta NTCP$ value is negative meaning that IMRT is more beneficial than IMPT.

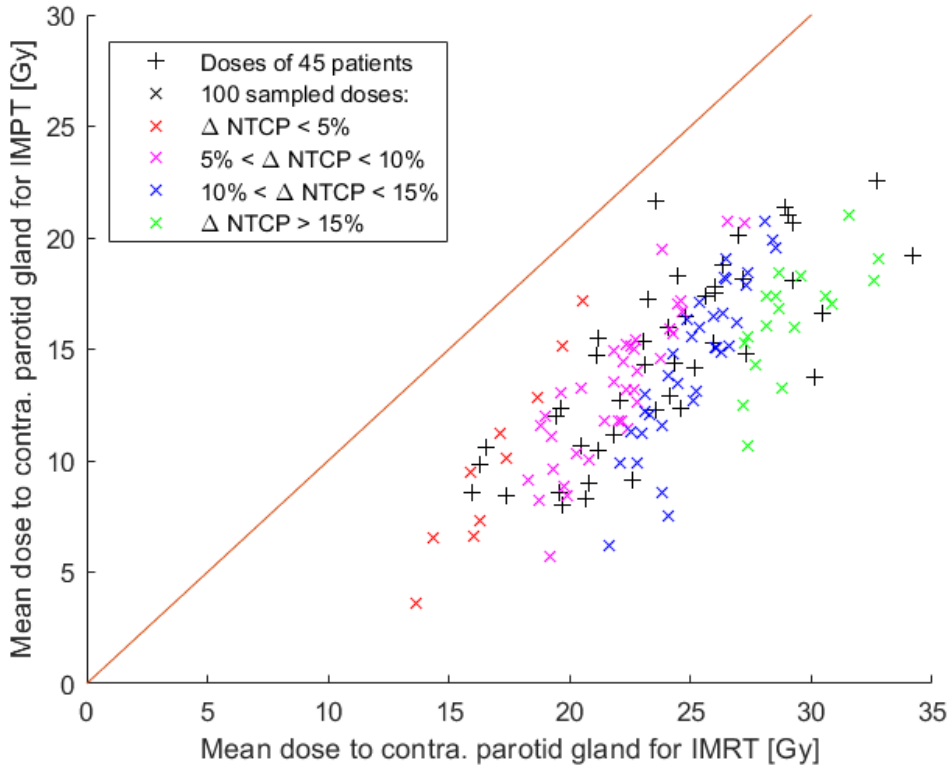

Figure 24 – Mean doses to contralateral parotid gland by photon and proton therapy of 45 HNSCC patients (+) and 100 samples (×) (simulated new HNSCC patients for 1 year). The linear red line indicates where the mean doses by IMRT and IMPT are the same.

7.2.2 Results for the clinical simulations

The simulations are performed with the SIB scheme and the NTCP model for xerostomia. For 11'200 working days and with 2 new HNSCC patients per week on average, a total of 4500 patients are treated. 4500 pair of mean doses are sampled and assigned to these patients. The $NTCP^{SIB}_{average}$ value for xerostomia is 16.9% and 6.3% if all the patients are treated with photons only and protons only, respectively.

1. Optimal $\Delta NTCP_{threshold}$ with 3 proton slots per day

The simulations for the threshold-based patient selection are carried out with $\Delta NTCP_{threshold}$ varied from 0% to 25% with 3 proton slots per day. The simulations are compared in terms of $NTCP^{SIB}_{Average}$ values to determinate the optimal $\Delta NTCP_{threshold}$ (Fig. 25).

The $\Delta NTCP_{threshold}$ value which minimizes the $NTCP^{SIB}_{average}$ for the 4500 simulated HNSCC patients is 11%. In the results below, a 10% $\Delta NTCP_{threshold}$ for xerostomia is since this represents the threshold proposed in the dutch PT patient selection scheme (see section 2.3) and the difference between a 10% and 11% threshold is small.

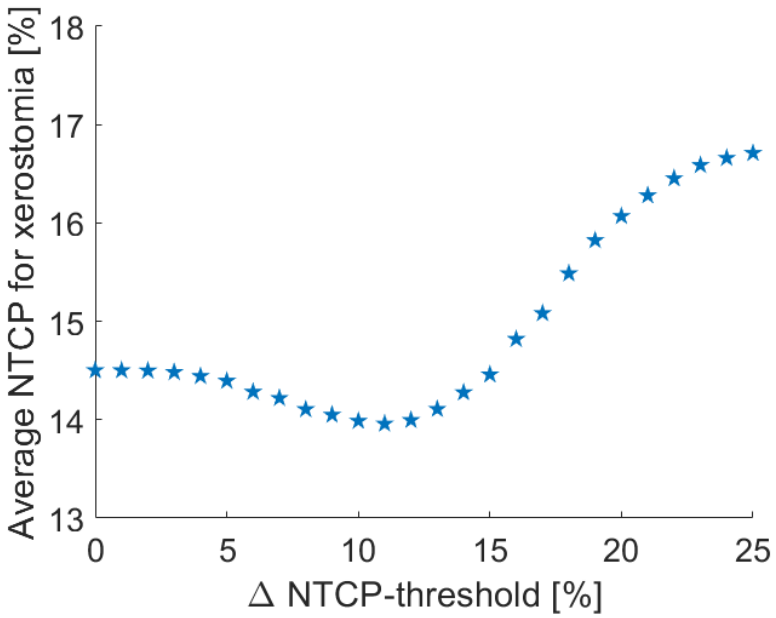

Figure 25 – $NTCP^{SIB}_{Average}$ values as function of the $\Delta NTCP_{threshold}$ for the patient selection based on xerostomia's model

2. Allocation of proton and photon fractions with 3 proton slots per day

Two simulations with 3 proton slots per day are performed for the daily slot allocation strategy and the threshold-based patient selection. The Table 8 lists the number of patients who receive IMRT, IMPT and combined treatment for each scenario. For the daily slot allocation strategy, 56% of the patients receive at least one proton fraction and 2% of the patients are assigned to pure IMPT. For the threshold-based selection, 20% of the patients are assigned to pure IMPT. The histogram in Figure 26 illustrates how many proton fractions patients receive in combined and only IMPT treatments. For example, 131 out of 2506 patients received exactly 10 proton fractions. Also, 85 patients received 30 proton fractions, including all patients with a very large $\Delta NTCP$.

Table 8 – Number of patients (and percentage) who receive IMRT, IMPT or combined treatment for a simulation with 11'200 days and 4500 patients for the daily slot allocation and threshold-based patient selection.

	Daily slot allocation	Patient selection
Only IMRT	1994 (44%)	3579 (80%)
Only IMPT	85 (2%)	921 (20%)
Combined treatment	2421 (54%)	0

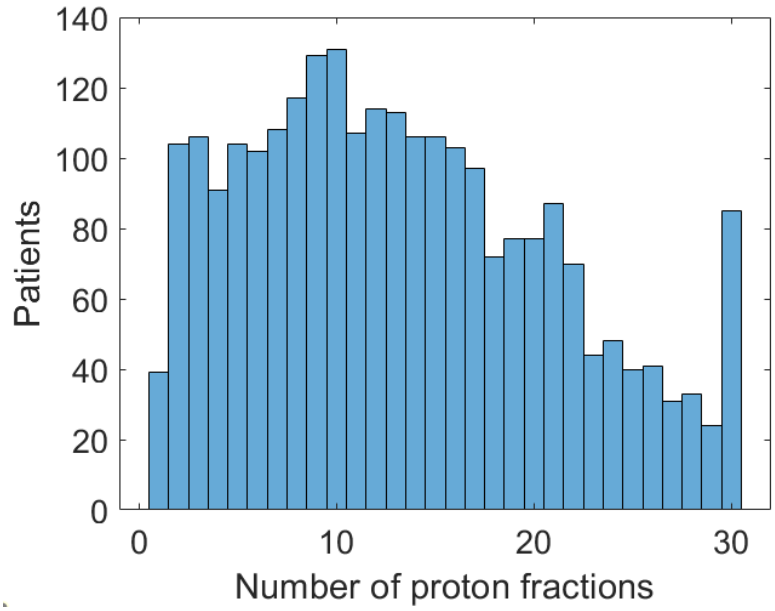

Figure 26 – Distribution of proton fractions over the 2506 patients who receive combined treatment and only IMPT in the daily slot allocation strategy

The allocation of proton and photon slots for 100 simulated HNSCC patients with three proton slots per day are shown in Figure 27 for the daily slot allocation and in Figure 28 for the threshold-based patient selection. These 100 simulated HNSCC patients are taken after the first 400 days of the simulation. Each time a patient receives a proton fraction, a checkbox is colored.

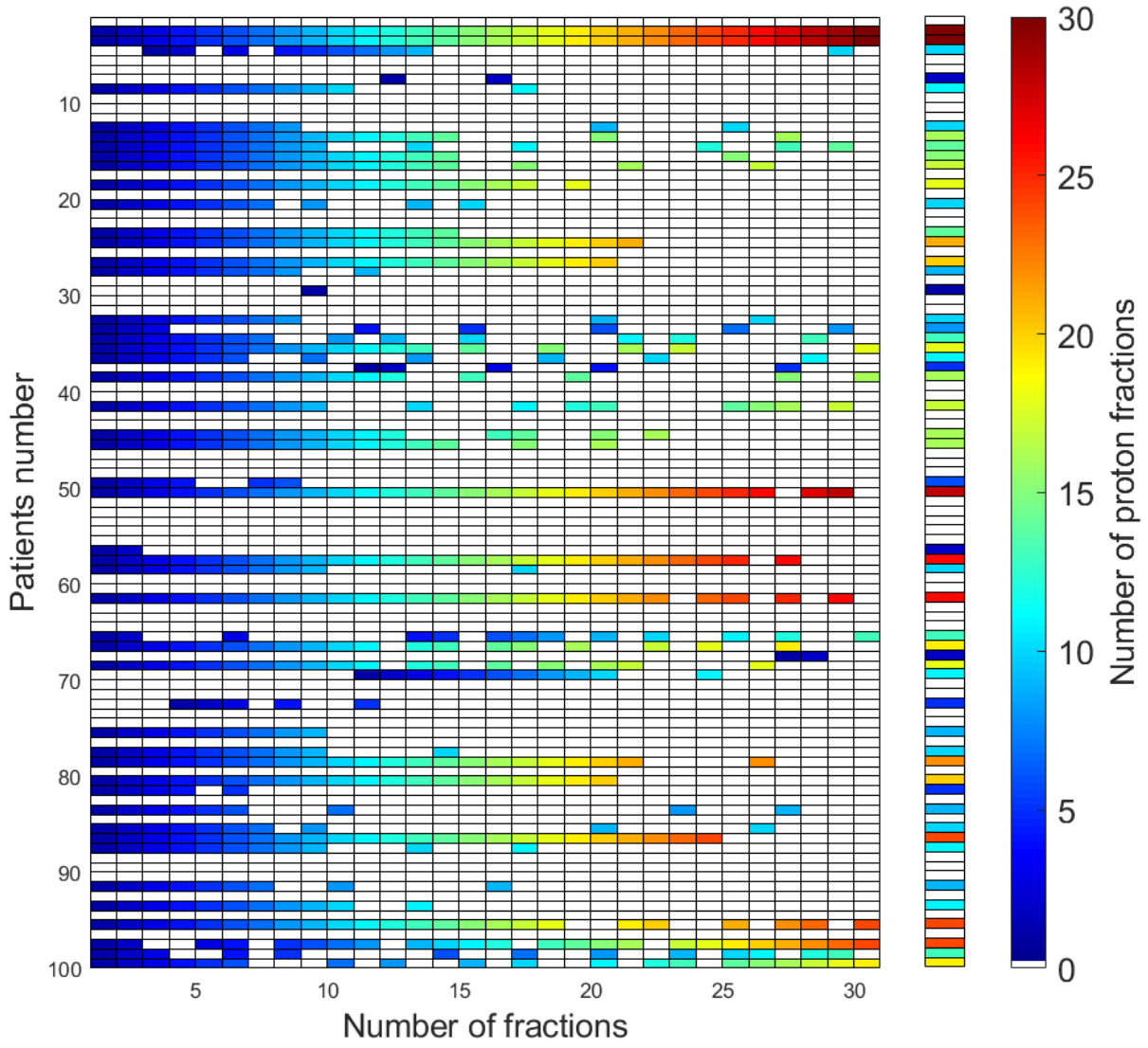

Figure 27 – Allocation of proton and photon slots for 100 patients for the daily slot allocation. The total number of proton slots per patient is illustrated in the last column.

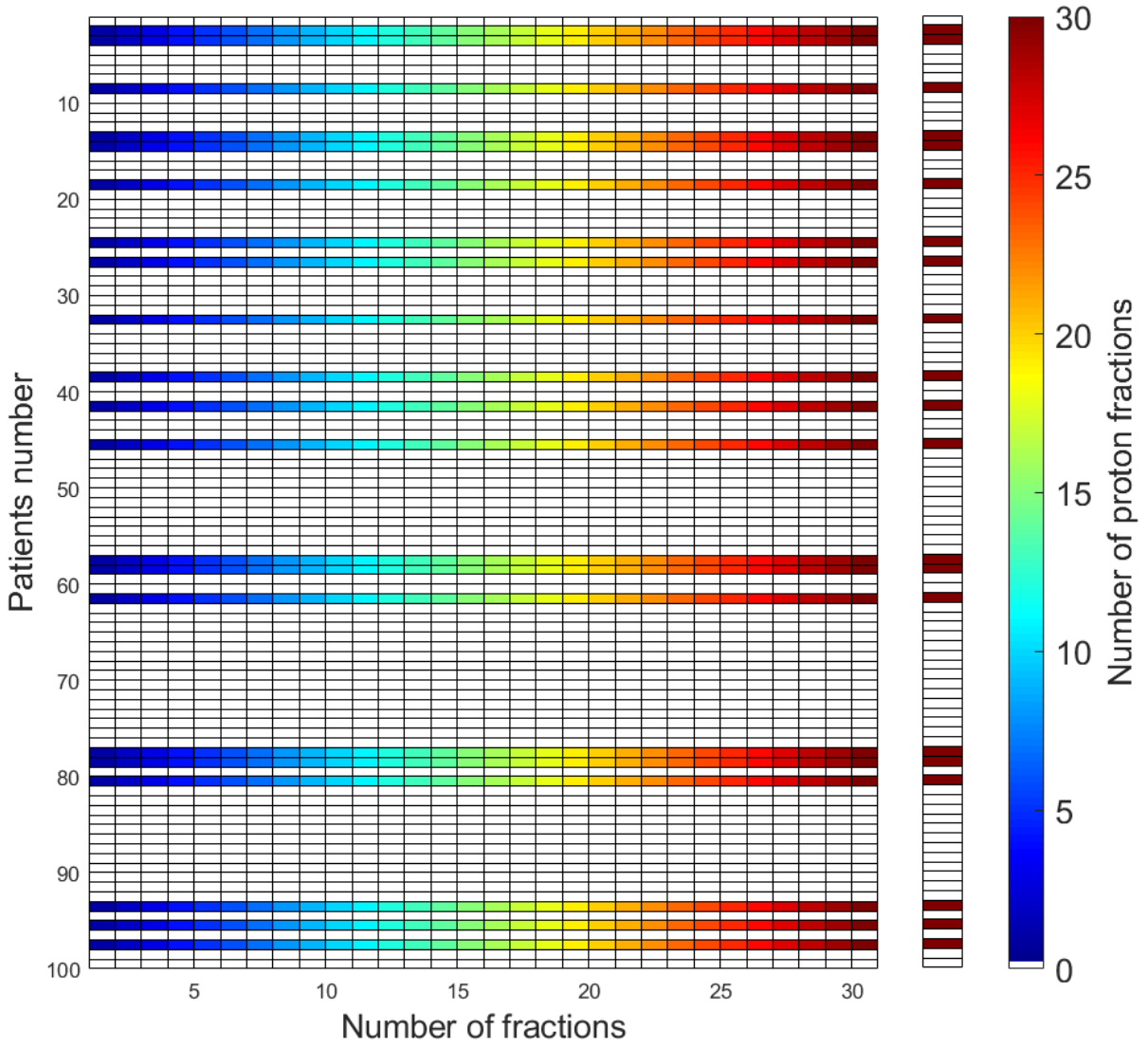

Figure 28 – Allocation of proton and photon slots for 100 patients for the threshold-based patient selection. The total number of proton slots per patient is illustrated in the last column.

For the daily slot allocation strategy (Fig. 27), 2 patients receive pure IMPT and 51 patients receive a combined treatment. All the proton fractions are used but are sparsely distributed.

Here, 768 proton slots are allocated over 100 patients. For the threshold-based patient selection (Fig. 28), 21 patients receive pure IMPT. Here, 630 proton fractions are used. In this scenario, 138 proton fractions are unused as a result of waiting for a patient with a $\Delta NTCP$ for xerostomia higher than 10% to come in the clinic. Also, some patients who have a $\Delta NTCP$ for xerostomia higher than 10% don't benefit from IMPT because all the proton slots were blocked on the day they presented.

3. Simulations of proton slot allocation with 1 to 10 proton slots per day

The simulations are performed for the daily slot allocation strategy and for the threshold-based patient selection with $\Delta NTCP_{threshold}$ of 5% , 10% and 15%. The number of fractions available per day varies from 1 to 10. The $NTCP^{SIB}_{average}$ values as function of the number of proton slots available are shown in Figure 29.

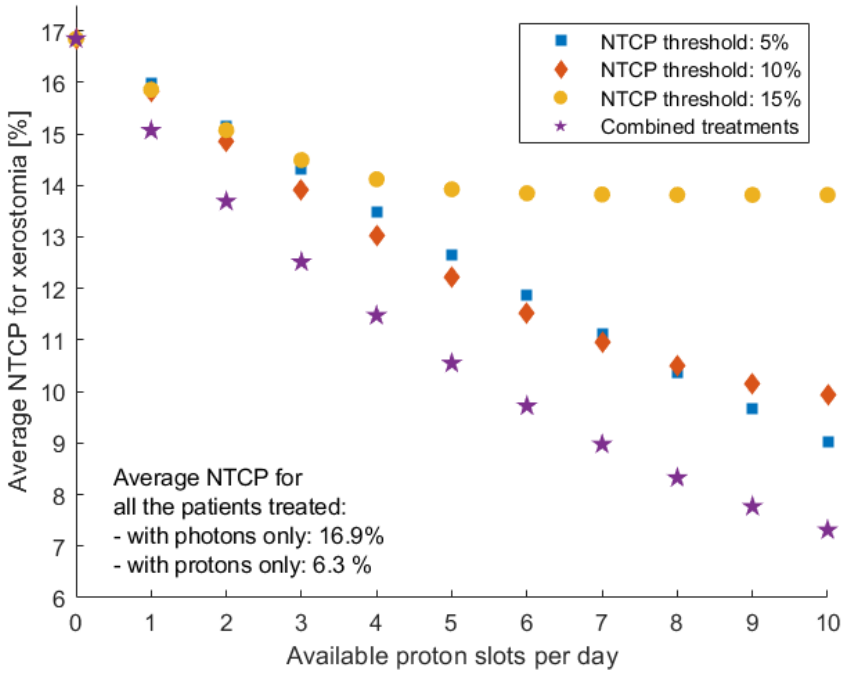

Figure 29 – The $NTCP_{average}$ for xerostomia as a function of the daily available proton slots for the combined treatment (daily slot allocation strategy) and the single-modality treatment (patient selection)

7.3 Comments

- The daily slot allocation strategy leads to a reduction of the $NTCP_{average}$ values for xerostomia compared to the threshold-based PT patient selection for any number of available proton slot per day (Fig. 29). If 3 proton slots are available per day for HNSCC patients, the $NTCP_{average}$ for xerostomia is 12.5% for the daily slot allocation strategy and 14.0% for the threshold-based PT patient selection which would select patients with 10% $\Delta NTCP_{threshold}$. The NTCP benefit of 1.5% can be explained by two considerations: 1) combined proton-photon treatments make optimal use of all proton slots whereas patient selection strategies face a trade-off between leaving slots unused or blocking slots for future patients with higher benefit; 2) on the convex part of the NTCP curve, the first proton fractions delivered are the most beneficial.

- From 1 to 7 proton slots available per day, the 10% $\Delta NTCP_{threshold}$ for the single-modality treatment is better than a threshold of 5% or 15%. The $NTCP_{average}$ is approximately constant for the 15% $\Delta NTCP_{threshold}$ for more than 5 proton slots per day. In this case, some proton slots are unused because not enough patients have a $\Delta NTCP$ value higher than 15% to fill all available proton slots. From 8 proton slots per day, the 5% threshold for the single-modality strategy becomes better than the 10% threshold, because there are enough proton resources to treat all the patients.

8 Outlook

In chapter 7, only one toxicity (xerostomia) was investigated to maximize the benefit of combined treatment for the continuous operation of a clinic over time. This work can be extend by considering another toxicity such as dysphagia. The NTCP model for dysphagia depends on the mean doses to the supraglottic and the superior PCM. The individual $\Delta NTCP$ for xerostomia and dysphagia for a patient j ($\Delta NTCP_j^{Xero}$, $\Delta NTCP_j^{Dysphagia}$) or the sum of the two toxicities $\Delta NTCP_j^{sum}$ (Eq. 36) could be considered in the daily slot allocation strategy to distribute optimally the available proton slots.

$$\Delta NTCP_j^{sum} = \Delta NTCP_j^{Xero} + \Delta NTCP_j^{Dysphagia} \tag{36}$$

To generate a large cohort with NTCP values for dysphagia and xerostomia, the proton and photon mean doses in the supraglottic, the superior PCM and the contralateral parotid gland would be sampled from a 6D Gaussian distribution.

Moreover, the daily slot allocation strategy represents an ideal situation in which all the proton slots available are used for a specific type of cancer. The negative point of this strategy is that the patients would only know if they receive a photon or proton fraction every morning. In contrast, the threshold-based patient selection approaches a clinical practice proposed in the dutch patient selection model (see section 2.3). With this patient selection model, not all the proton fractions are used. However, in reality, unused proton slots for HNSCC are used for other type of cancers. As an extension of this work, an intermediate scenario could be developed to make an optimal use of all proton slots while making it more practical than the daily slot allocation strategy. A scenario in which the patients are assigned to 0, 10, 20 or 30 proton fractions or a scenario in which the patients are assigned to proton slots on a weekly basis could be investigated.

9 Conclusion

Motivated by the potential benefit of PT over XT among cancer patients, we investigated optimal combined proton-photon radiotherapy in the context of limited proton fractions. We developed methods to optimally distribute those limited proton slots over a cohort of 45 HNSCC patients optimally in order to optimize the benefit of PT at a population level. We demonstrated that combined proton-photon treatments with an optimized allocation of proton slots decrease the average complication risks for specific NTCP models (e.g. xerostomia) at the population level. Stated differently, fewer proton fractions can be used to achieve an equivalent average complication risk on the population level compared to a patient-wise selection. Then, we considered a clinic offering both photons and protons and a scenario, in which only limited PT slots are available per day for treating HNC patients. An algorithm which optimally distributes the proton and the photon slots to HNSCC patients over time was developed for a daily slot allocation strategy and a threshold-based patient selection. The daily slot allocation strategy makes optimal use of all limited proton slots and increases the benefit of PT on the population level compared to a threshold-based patient selection. In conclusion, from a global health system perspective, limited proton therapy resources can be more efficiently used with combined proton-photon treatments and a daily proton slot allocation rather than single-modality treatments with optimal patient selection.

Bibliography

[1] E. Podgorsak and K. Kainz, *Radiation oncology physics: A handbook for teachers and students*. International Atomic Energy Agency, 2005.

[2] H. Fritz-Niggli, *Strahlengefährdung, Strahlenschutz: ein Leitfaden für die Praxis*. Huber, 1991.

[3] D. M. Soliman, "Augmented microscopy: development and application of high-resolution optoacoustic and multimodal imaging techniques for label-free biological observation," PhD thesis, Technische Universitaet Muenchen, 2017.

[4] H. Paganetti, *Proton Therapy Physics*. Boca Raton: CRC Press, 2012.

[5] W. D. Newhauser and R. Zhang, "The physics of proton therapy," *Physics in Medicine & Biology*, vol. 60, no. 8, R155, 2015.

[6] A. Lagzda, R. Jones, J. Jones, K. Kirkby, W. Farabolini, and D. Angal-Kalinin, "Relative insensitivity to inhomogeneities on very high energy electron dose distributions," 2017.

[7] I. C. on Radiation Units, *Prescribing, recording, and reporting photon beam therapy*. International Commission on Radiation, 1993, vol. 50.

[8] I. C. on Radiation Units and Measurements, *ICRU Report 62*. Oxford University Press Bethesda, 1999.

[9] T. Bortfeld, "Imrt: a review and preview," *Physics in Medicine & Biology*, vol. 51, no. 13, R363, 2006.

[10] H. E. Romeijn, R. K. Ahuja, J. F. Dempsey, and A. Kumar, "A column generation approach to radiation therapy treatment planning using aperture modulation," *SIAM Journal on Optimization*, vol. 15, no. 3, pp. 838–862, 2005.

[11] E. Rosenblatt, J. Izewska, Y. Anacak, Y. Pynda, P. Scalliet, M. Boniol, and P. Autier, "Radiotherapy capacity in european countries: an analysis of the directory of radiotherapy centres (dirac) database," *The lancet oncology*, vol. 14, no. 2, e79–e86, 2013.

[12] P. S. Institute. (2020). Spot scanning, [Online]. Available: `https://www.psi.ch/de/protontherapy/spot-scanning` (visited on 02/28/2020).

[13] A. J. Lomax, E. Pedroni, H. P. Rutz, and G. Goitein, "The clinical potential of intensity modulated proton therapy," *Zeitschrift für Medizinische Physik*, vol. 14, no. 3, pp. 147–152, 2004.

[14] A. Lomax, "Intensity modulation methods for proton radiotherapy," *Physics in Medicine & Biology*, vol. 44, no. 1, p. 185, 1999.

[15] PTCOG. (2020). Particle therapy co-operative group website, [Online]. Available: `https://www.ptcog.ch` (visited on 02/22/2020).

[16] T. R. Bortfeld and J. S. Loeffler, "Three ways to make proton therapy affordable," *Nature News*, vol. 549, no. 7673, p. 451, 2017.

[17] T. Bortfeld. (2019). Physics in the fight against cancer, [Online]. Available: `http://www.ias.uwa.edu.au/lectures/bortfeld` (visited on 02/22/2020).

[18] E. E. Vokes, R. R. Weichselbaum, S. M. Lippman, and W. K. Hong, "Head and neck cancer," *New England Journal of Medicine*, vol. 328, no. 3, pp. 184–194, 1993.

[19] C. R. Leemans, B. J. Braakhuis, and R. H. Brakenhoff, "The molecular biology of head and neck cancer," *Nature reviews cancer*, vol. 11, no. 1, pp. 9–22, 2011.

[20] J. Ferlay, I. Soerjomataram, R. Dikshit, S. Eser, C. Mathers, M. Rebelo, D. M. Parkin, D. Forman, and F. Bray, "Cancer incidence and mortality worldwide: sources, methods and major patterns in globocan 2012," *International journal of cancer*, vol. 136, no. 5, E359–E386, 2015.

[21] C. R. Leemans, P. J. Snijders, and R. H. Brakenhoff, "The molecular landscape of head and neck cancer," *Nature Reviews Cancer*, vol. 18, no. 5, p. 269, 2018.

[22] A. Argiris, M. V. Karamouzis, D. Raben, and R. L. Ferris, "Head and neck cancer," *The Lancet*, vol. 371, no. 9625, pp. 1695–1709, 2008.

[23] M. Steneker, A. Lomax, and U. Schneider, "Intensity modulated photon and proton therapy for the treatment of head and neck tumors," *Radiotherapy and oncology*, vol. 80, no. 2, pp. 263–267, 2006.

[24] T. A. van de Water, H. P. Bijl, C. Schilstra, M. Pijls-Johannesma, and J. A. Langendijk, "The potential benefit of radiotherapy with protons in head and neck cancer with respect to normal tissue sparing: a systematic review of literature," *The oncologist*, vol. 16, no. 3, p. 366, 2011.

[25] A. J. Lomax, M. Goitein, and J. Adams, "Intensity modulation in radiotherapy: photons versus protons in the paranasal sinus," *Radiotherapy and oncology*, vol. 66, no. 1, pp. 11–18, 2003.

[26] A. C. Moreno, S. J. Frank, A. S. Garden, D. I. Rosenthal, C. D. Fuller, G. B. Gunn, J. P. Reddy, W. H. Morrison, T. D. Williamson, E. B. Holliday, *et al.*, "Intensity modulated proton therapy (impt)–the future of imrt for head and neck cancer," *Oral oncology*, vol. 88, pp. 66–74, 2019.

[27] A. Jakobi, K. Stützer, A. Bandurska-Luque, S. Löck, R. Haase, L.-J. Wack, D. Mönnich, D. Thorwarth, D. Perez, A. Lühr, *et al.*, "Ntcp reduction for advanced head and neck cancer patients using proton therapy for complete or sequential boost treatment versus photon therapy," *Acta Oncologica*, vol. 54, no. 9, pp. 1658–1664, 2015.

[28] A. C. Houweling, M. E. Philippens, T. Dijkema, J. M. Roesink, C. H. Terhaard, C. Schilstra, R. K. Ten Haken, A. Eisbruch, and C. P. Raaijmakers, "A comparison of dose–response models for the parotid gland in a large group of head-and-neck cancer patients," *International Journal of Radiation Oncology Biology Physics*, vol. 76, no. 4, pp. 1259–1265, 2010.

[29] A. Peeters, J. P. Grutters, M. Pijls-Johannesma, S. Reimoser, D. De Ruysscher, J. L. Severens, M. A. Joore, and P. Lambin, "How costly is particle therapy? cost analysis of external beam radiotherapy with carbon-ions, protons and photons," *Radiotherapy and oncology*, vol. 95, no. 1, pp. 45–53, 2010.

[30] J. A. Langendijk, P. Lambin, D. De Ruysscher, J. Widder, M. Bos, and M. Verheij, "Selection of patients for radiotherapy with protons aiming at reduction of side effects: the model-based approach," *Radiotherapy and Oncology*, vol. 107, no. 3, pp. 267–273, 2013.

[31] Landelijk-Platform-Protonentherapie, "Landelijk indicatie protocol protonen therapie hoofd-halstumoren," p. 70, 2017.

[32] S. E. Combs and J. Debus, "Treatment with heavy charged particles: systematic review of clinical data and current clinical (comparative) trials," *Acta Oncologica*, vol. 52, no. 7, pp. 1272–1286, 2013.

[33] S. C. ten Eikelder, D. den Hertog, T. R. Bortfeld, and Z. Perkó, "Optimal combined proton-photon therapy schemes based on the standard bed model," *Physics in medicine and biology*, 2019.

[34] J. Unkelbach, M. Bangert, K. D. A. Bernstein, N. Andratschke, and M. Guckenberger, "Optimization of combined proton–photon treatments," *Radiotherapy and Oncology*, vol. 128, no. 1, pp. 133–138, 2018.

[35] H. Gao, "Hybrid proton-photon inverse optimization with uniformity-regularized proton and photon target dose," *Physics in Medicine & Biology*, vol. 64, no. 10, p. 105 003, 2019.

[36] S. Fabiano, P. Balermpas, M. Guckenberger, and J. Unkelbach, "Combined proton–photon treatments–a new approach to proton therapy without a gantry," *Radiotherapy and Oncology*, vol. 145, pp. 81–87, 2020.

[37] A. Jakobi, A. Lühr, K. Stützer, A. Bandurska-Luque, S. Löck, M. Krause, M. Baumann, R. Perrin, and C. Richter, "Increase in tumor control and normal tissue complication probabilities in advanced head-and-neck cancer for dose-escalated intensity-modulated photon and proton therapy," *Frontiers in oncology*, vol. 5, p. 256, 2015.

[38] A. Jakobi, A. Bandurska-Luque, K. Stützer, R. Haase, S. Löck, L.-J. Wack, D. Mönnich, D. Thorwarth, D. Perez, A. Lühr, *et al.*, "Identification of patient benefit from proton therapy for advanced head and neck cancer patients based on individual and subgroup normal tissue complication probability analysis," *International Journal of Radiation Oncology Biology Physics*, vol. 92, no. 5, pp. 1165–1174, 2015.

[39] L. B. Marks, E. D. Yorke, A. Jackson, R. K. Ten Haken, L. S. Constine, A. Eisbruch, S. M. Bentzen, J. Nam, and J. O. Deasy, "Use of normal tissue complication probability models in the clinic," *International Journal of Radiation Oncology Biology Physics*, vol. 76, no. 3, S10–S19, 2010.

[40] J. T. Lyman and A. B. Wolbarst, "Optimization of radiation therapy, iii: a method of assessing complication probabilities from dose-volume histograms," *International Journal of Radiation Oncology Biology Physics*, vol. 13, no. 1, pp. 103–109, 1987.

[41] A. Eisbruch, H. M. Kim, F. Y. Feng, T. H. Lyden, M. J. Haxer, M. Feng, F. P. Worden, C. R. Bradford, M. E. Prince, J. S. Moyer, *et al.*, "Chemo-imrt of oropharyngeal cancer aiming to reduce dysphagia: swallowing organs late complication probabilities and dosimetric correlates," *International Journal of Radiation Oncology Biology Physics*, vol. 81, no. 3, e93–e99, 2011.

[42] M. E. Christianen, C. Schilstra, I. Beetz, C. T. Muijs, O. Chouvalova, F. R. Burlage, P. Doornaert, P. W. Koken, C. R. Leemans, R. N. Rinkel, *et al.*, "Predictive modelling for swallowing dysfunction after primary (chemo) radiation: results of a prospective observational study," *Radiotherapy and Oncology*, vol. 105, no. 1, pp. 107–114, 2012.

[43] S. A. Bhide, S. Gulliford, U. Schick, A. Miah, S. Zaidi, K. Newbold, C. M. Nutting, and K. J. Harrington, "Dose–response analysis of acute oral mucositis and pharyngeal dysphagia in patients receiving induction chemotherapy followed by concomitant chemo-imrt for head and neck cancer," *Radiotherapy and Oncology*, vol. 103, no. 1, pp. 88–91, 2012.

Acknowledgements

I would like to thank Prof. Dr. Jan Unkelbach for giving me the opportunity to realize my master thesis in the physics research group of the Department of Radiation Oncology at the Zürich University Hospital. I particularly appreciate his permanent availability, his guidance and precious advice which contributed to my thinking. I would like to thank him for reviewing in a short amount of time the final version of the thesis.

I am very grateful to Silvia Fabiano who coached me throughout this thesis. I would like to thank her for her sound advice, enthusiasm, kindness, friendship and finally for reviewing all chapters of this thesis.

I am delighted to have worked closely with Prof. Dr. Jan Unkelbach and Silvia Fabiano, because in addition to their scientific support, they were always ready to advise me during the development of this thesis.

This work could not have been carried out without the data set provided by Dr. Kristin Stützer, Dr. Christian Richter, Dr. Annika Jakobi and Dr. Anna Bandurska-Luque. I would like to thank particularly Dr. Kristin Stützer and Dr. Christian Richter for their precious cooperation, for taking time to answer my questions and giving us the opportunity to present the results of this thesis at their institution in Dresden.

I would like to thank Dr. Dávid Papp for sharing his expertise and guidance to develop mathematical optimization algorithms.

My last thanks go to my parents Katia and Jean-Luc and my sister Viviane for their moral and material support and their unfailing confidence in my choices.

Annexes

A The doses to the contralateral parotid gland for the 45 HNSCC patients

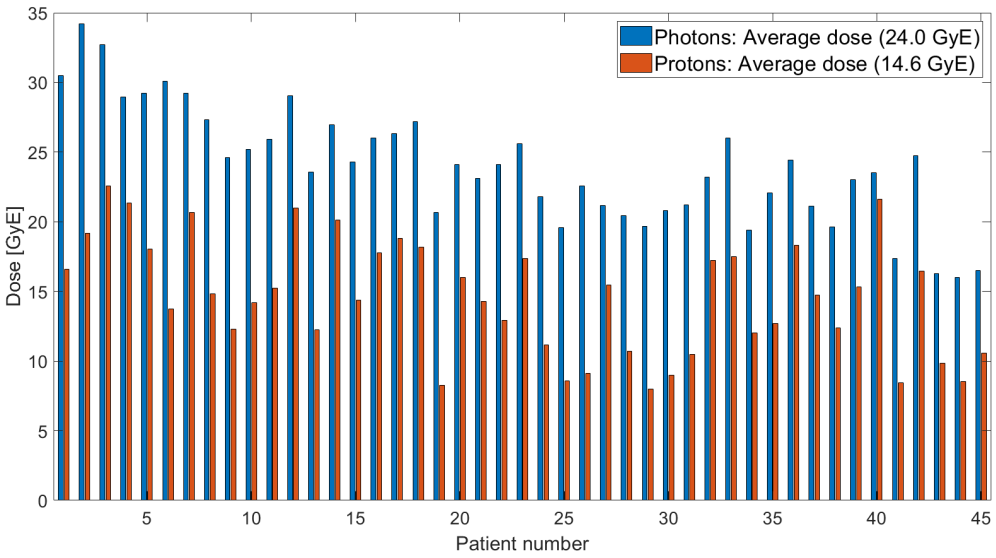

(a) SIB scheme

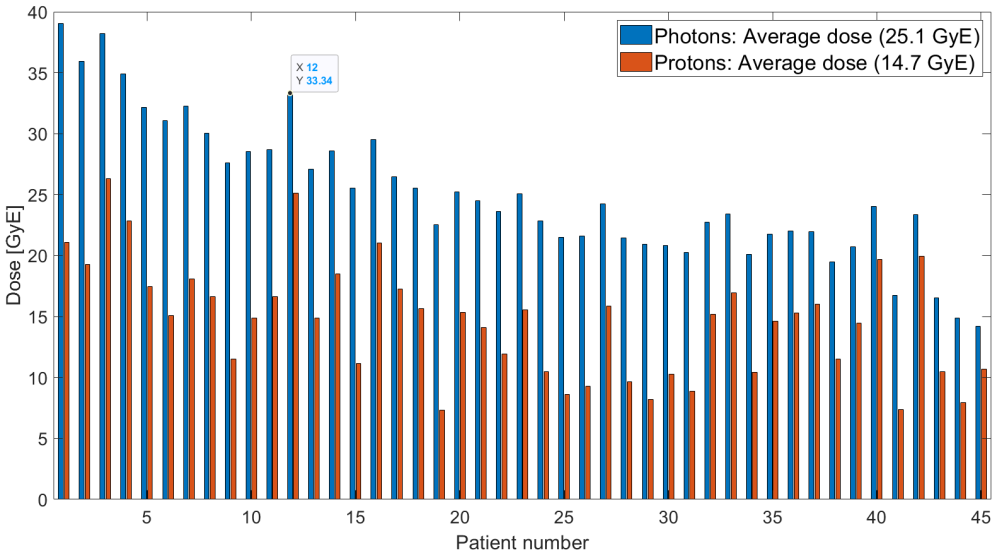

(b) SEQ scheme

B Boxplots for the NTCP models for dysphagia, larynx-based aspiration, PCM-based aspiration, acute mucositis for HN-SCC patients

A) Dysphagia

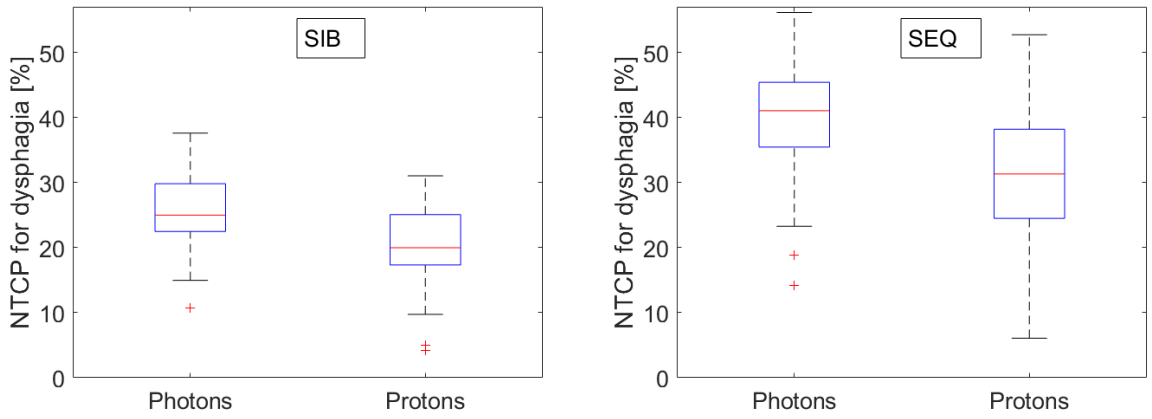

B) Larynx-based aspiration

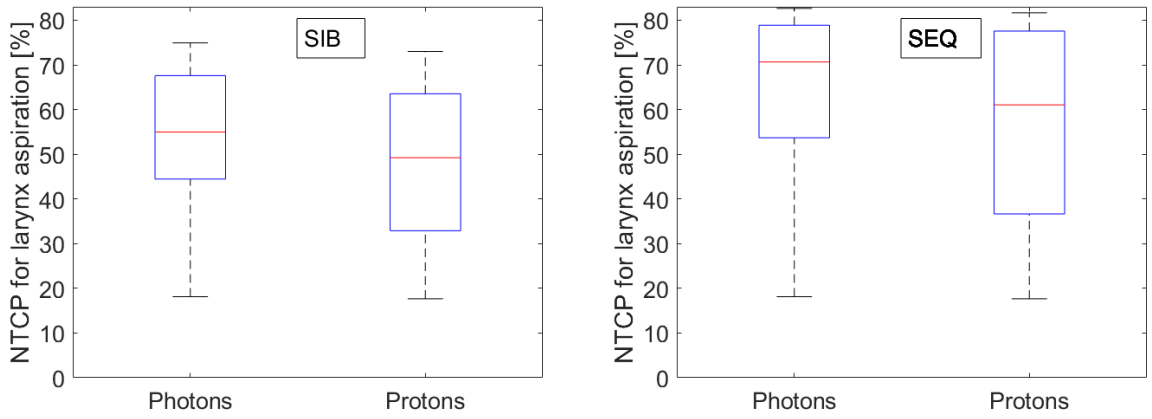

C) PCM-based aspiration

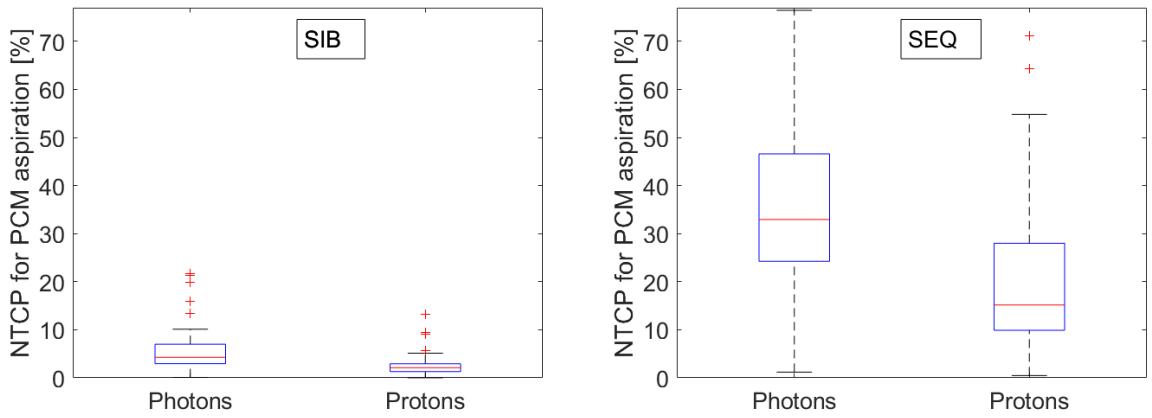

D) Acute mucositis

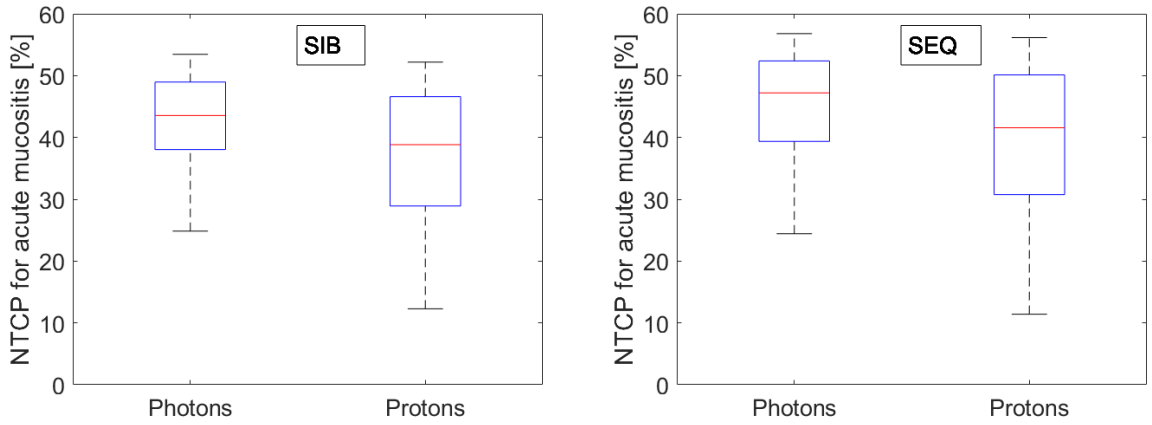

C Acute mucositis: Optimal allocation for 20% of proton slots

Note: The ordering of patients is identical to Fig. 19.

a) SIB scheme: The allocation for the fraction-wise and patient-wise selection are the same

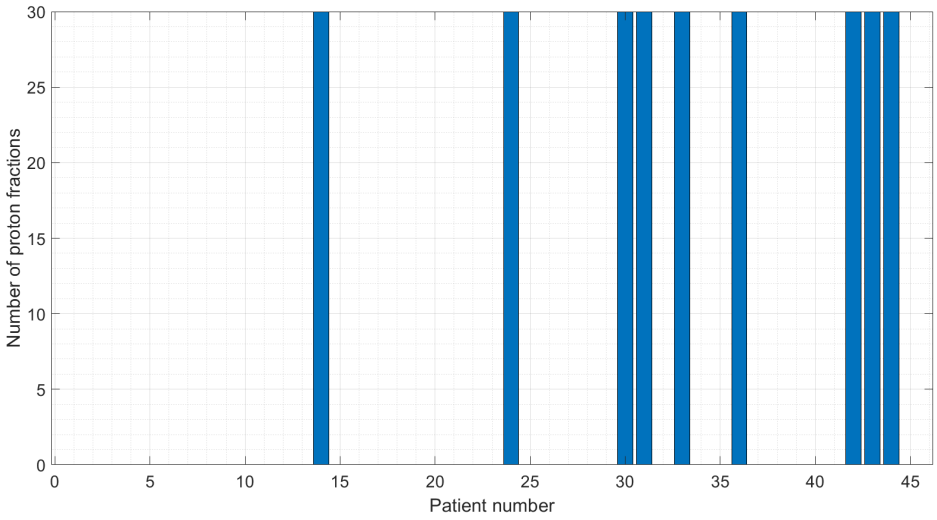

b) SEQ scheme: Allocation for the fraction-wise selection

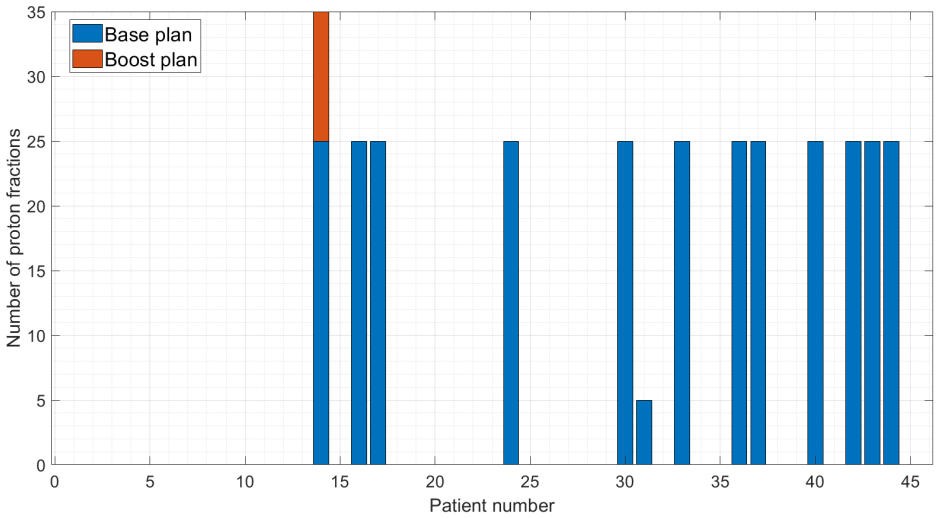

c) SEQ scheme: Allocation for the patient-wise selection

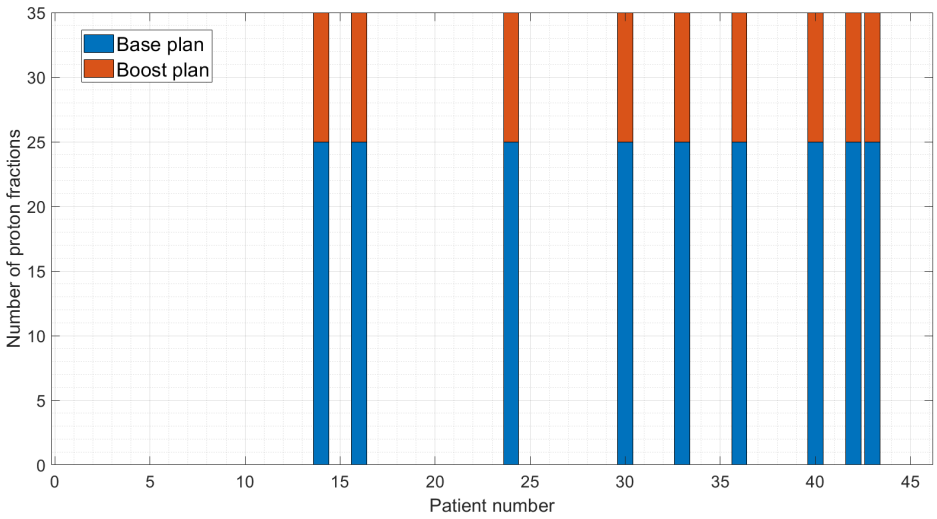

D $NTCP_{average}$ for a range of proton slots

The $NTCP_{average}$ values for dysphagia, larynx-based aspiration, PCM-based aspiration, acute mucositis for HNSCC patients.

A) Dysphagia

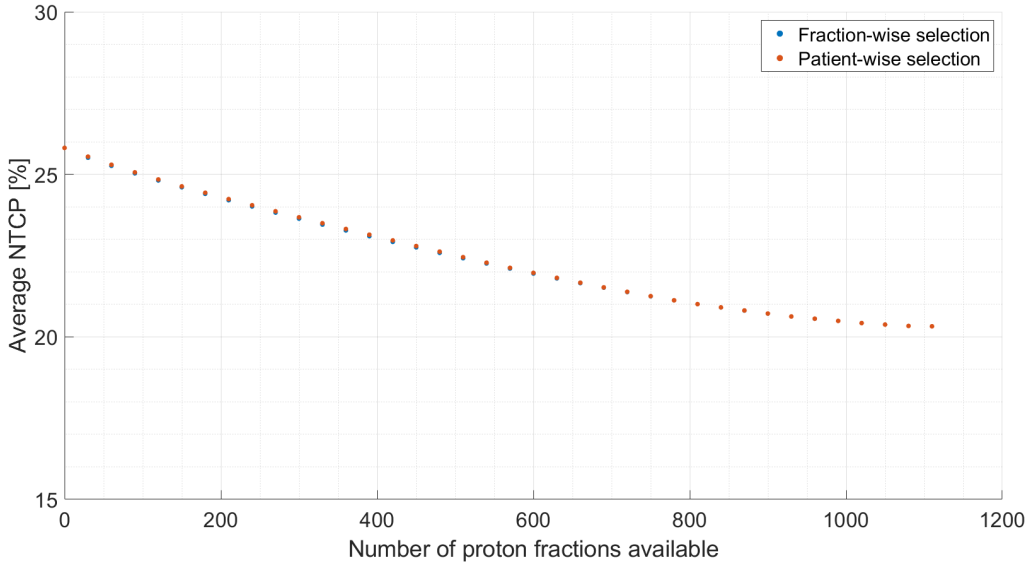

(a) SIB scheme

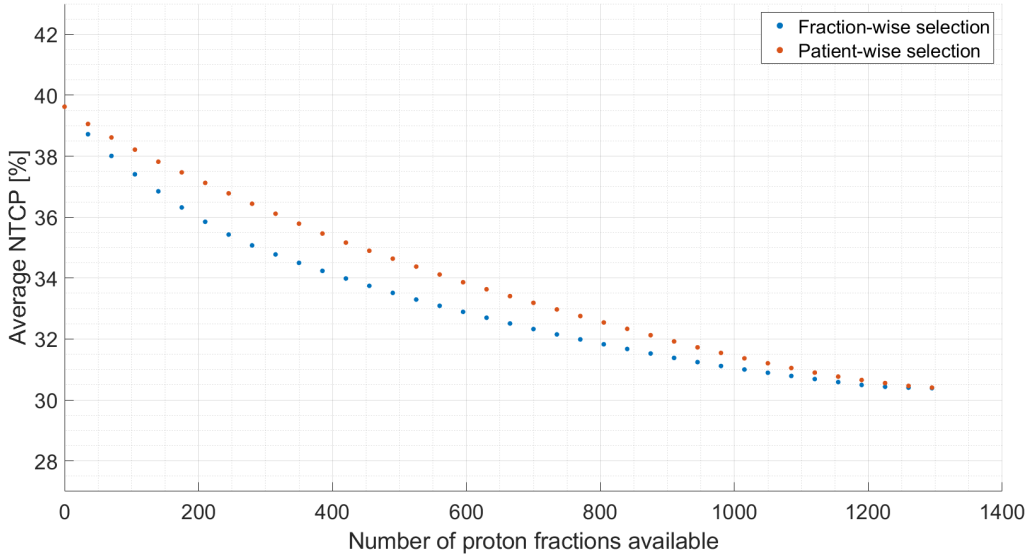

(b) SEQ scheme

B) Larynx-based aspiration

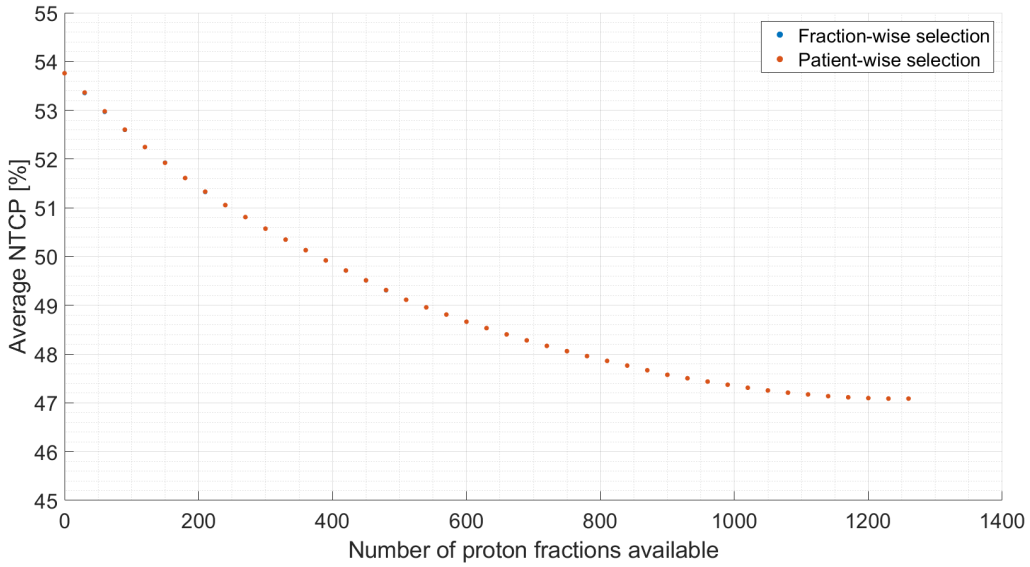

(a) SIB scheme

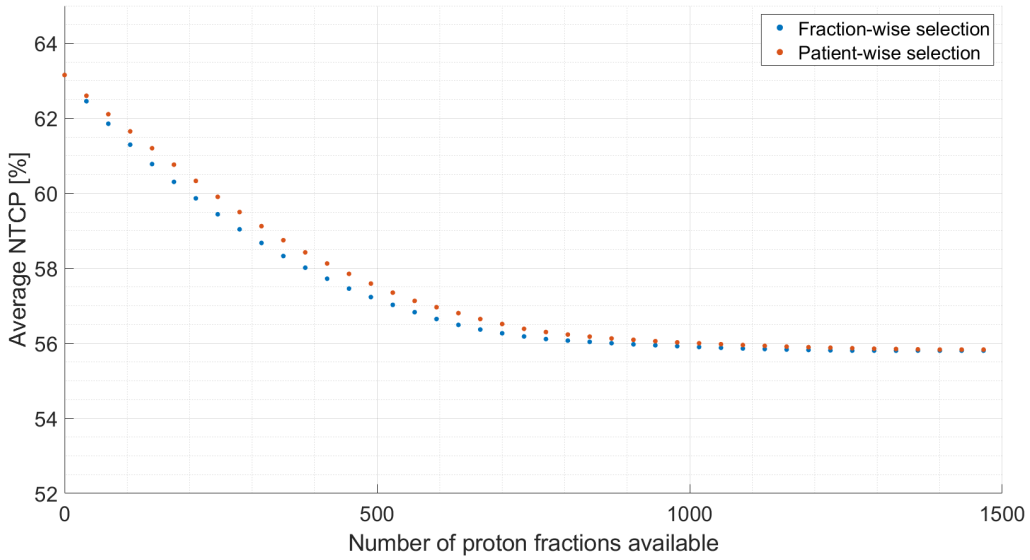

(b) SEQ scheme

C) PCM-based aspiration

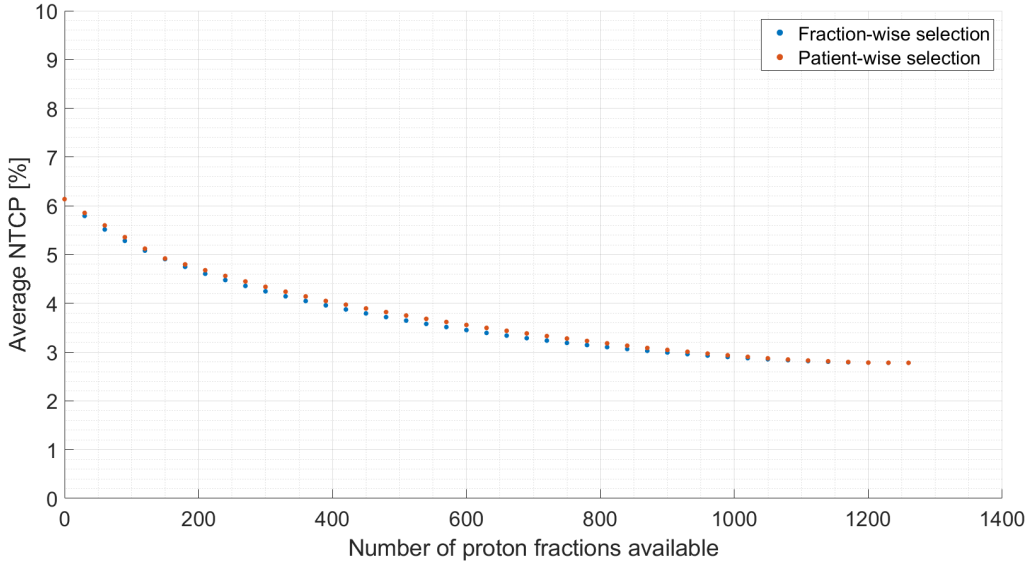

(a) SIB scheme

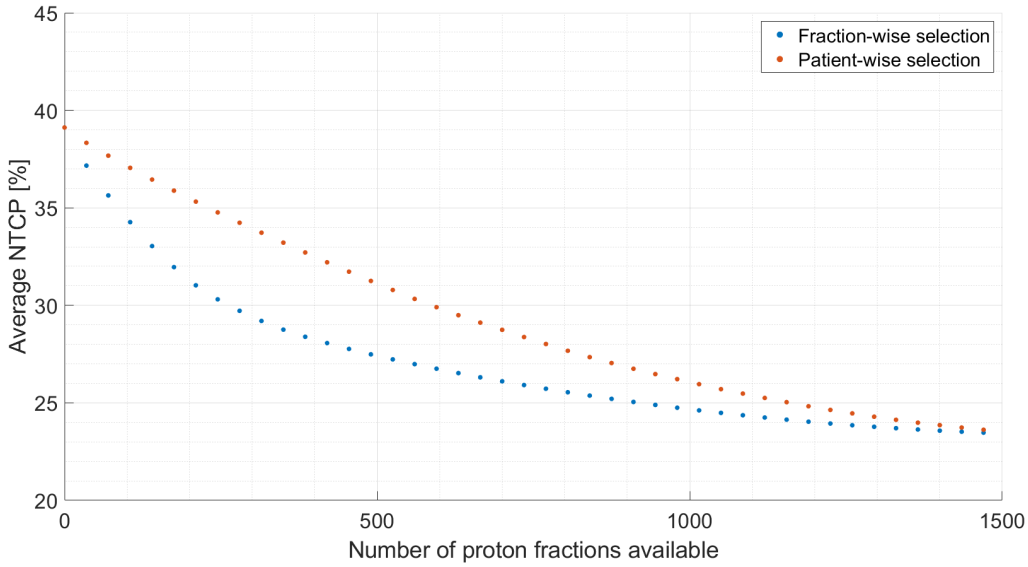

(b) SEQ scheme

D) Acute mucositis

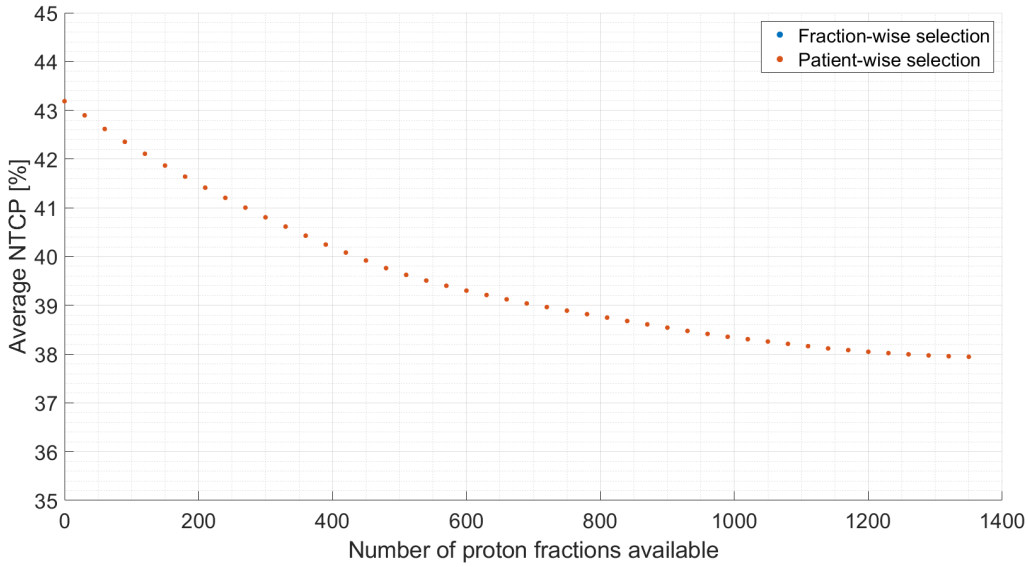

(a) SIB scheme

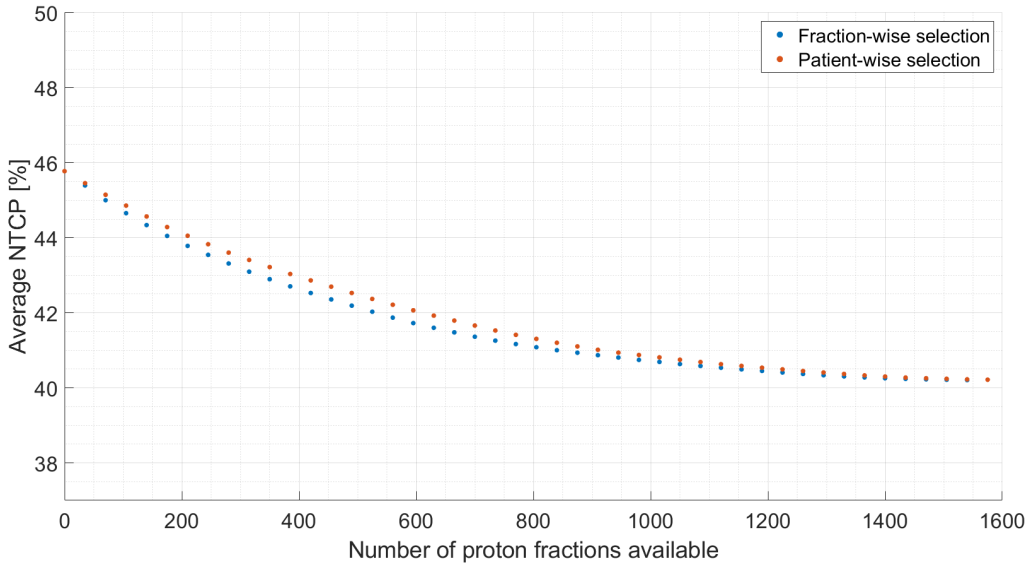

(b) SEQ scheme